# An environmentally-aware dynamic planning of electric vehicles for aircraft towing considering stochastic aircraft arrival and departure times

van Oosterom, Simon; Mitici, Mihaela

**DOI**
10.1016/j.trc.2024.104857

**Publication date**
2024

**Document Version**
Final published version

**Published in**
Transportation Research Part C: Emerging Technologies

**Citation (APA)**
van Oosterom, S., & Mitici, M. (2024). An environmentally-aware dynamic planning of electric vehicles for aircraft towing considering stochastic aircraft arrival and departure times. *Transportation Research Part C: Emerging Technologies*, *169*, Article 104857. https://doi.org/10.1016/j.trc.2024.104857

Transportation Research Part C 169 (2024) 104857

Contents lists available at ScienceDirect

Transportation Research Part C

journal homepage: www.elsevier.com/locate/trc

# An environmentally-aware dynamic planning of electric vehicles for aircraft towing considering stochastic aircraft arrival and departure times

Simon van Oosterom [a,*], Mihaela Mitici [b]

[a] Faculty of Aerospace Engineering, Delft University of Technology, Kluyverweg 1, HS 2926 Delft, The Netherlands
[b] Faculty of Science, Utrecht University, Heidelberglaan 8, 3584 CS Utrecht, The Netherlands

ARTICLE INFO

*Keywords:*
Sustainable aviation
Electric towing vehicles
Vehicle routing problem
Dynamic scheduling
Stochastic scheduling

ABSTRACT

Introducing electric vehicles that tow aircraft during taxiing is an emerging technology aimed at supporting climate neutrality for aviation. Planning electric towing operations is, however, impeded by the high uncertainty in aircraft arrival and departure times. We address the question of how to plan the operation of a fleet of Electric Towing Vehicles (ETVs) to maximize environmental benefits, given the uncertainty in aircraft arrival/departure times. For this, we propose a stochastic and dynamic planning framework for ETVs, where stochastic aircraft arrival and departure times are updated during the day. With this, the assignment of the ETVs-to-aircraft to replace conventional taxiing, and ETV battery charging times are planned such that the fuel savings are maximized. At the same time, we ensure that aircraft delays induced by the use of ETVs are minimized. We illustrate our framework for a large European airport. The results show that our framework achieves 79.5% of the highest possible cost reduction (fuel and ETV-induced delay), which is obtained when full knowledge of the arrival/departure times is available in advance. Furthermore, we show that considering the uncertainty in the arrival/departure times, rather than using point estimates of these times, leads to a 17.7% additional cost reduction. Overall, our framework supports the implementation of electric aircraft towing with maximum environmental benefits while considering the dynamic, uncertain arrival and departure times of aircraft.

## 1. Introduction

The aviation industry is responsible for approximately 5% of the anthropomorphic climate impact (Lee et al., 2021). Because it is a *hard-to-abate* sector with fast growth of 5% annually (International Air Transport Association, 2022), this share is expected to increase in the coming years. Though the industry pledges to reduce its climate impact (United Nations Framework Convention on Climate Change, 2015), climate neutrality will take many more years. The most effective ways to reduce emissions, such as the use of synthetic kerosene, electric aircraft and alternative aircraft configurations, will not be ready for a full scale roll-out before 2035 (Ranasinghe et al., 2019). As such, in order to meet the challenge, improving operations using existing technology plays a vital part (Roosenbrand et al., 2023).

Introducing electric towing vehicles (ETVs) for aircraft to replace conventional aircraft taxing is a promising avenue to reduce aviation emissions (Khadilkar and Balakrishnan, 2012; Lukic et al., 2019). The deployment of these vehicles could reduce the CO2

* Corresponding author.
*E-mail address:* s.j.m.vanoosterom@tudelft.nl (S. van Oosterom).

https://doi.org/10.1016/j.trc.2024.104857
Received 8 March 2024; Received in revised form 9 September 2024; Accepted 13 September 2024
Available online 21 September 2024

emission during taxiing by 98% (Lukic et al., 2019). Even though the taxiing distance is relatively small compared with the entire flight, its climate impact is significant. In fact, by towing an aircraft to and from the runway with an electric towing vehicle, fuel savings of up to 6% on an average flight is achieved (Khadilkar and Balakrishnan, 2012; Nikoleris et al., 2011).

The expected environmental benefits of ETVs have incentivized the study of ETV planning in the last few years, see for example Soltani et al. (2020) and van Oosterom et al. (2022). ETV planning considers the problem of assigning ETVs to aircraft for towing, while leaving time for ETV battery charging throughout the day. Existing studies, however, assume that the exact flight arrival and departure times are known at the start of the day (Soltani et al., 2020; van Oosterom et al., 2022). With this, the schedule for the entire day can be globally optimized during the *tactical* planning phase. This is an idealized perspective. In practice, flights are constantly arriving/departing earlier or later than scheduled (see Section 3) (EUROCONTROL, 2023a,b). To address this, we plan the operations of ETVs while accounting for the uncertainty in aircraft arrival/departure times. For this, we use estimates of the arrival/departure times. These times are continuously updated as the aircraft approaches its actual landing or take-off.

In this paper, we propose a dynamic Electric Vehicle Routing Problem with Time Windows (E-VRP-TW) that plans the towing tasks and battery charging of a fleet of ETVs, taking into account the uncertainty in the aircraft arrival and departure times. These times and the associated uncertainties are updated over time as the aircraft come closer to the actual landing or take-off. Using a rolling horizon approach, the arrival/departure times are periodically updated and, in turn, the ETV planning is reevaluated. The objective of the ETV planning is to maximize the fuel savings due to the intelligent replacement of conventional taxiing with electric towing. At the same time, we ensure that flight delays induced by ETV operations are minimized. Together, these objectives define the cost reduction we aim to achieve by an intelligent planning of the ETVs. We illustrate our framework for electric towing of narrow-body aircraft at Amsterdam Airport Schiphol. Flight schedules during the summer and autumn of 2023 are considered, with an average of 998 flights per day. The distributions of the aircraft arrival and departure times are obtained based on historical flight schedules. The results show that an average cost reduction (fuel and ETV-induced delay costs) of €12 104 per ETV per day is achieved, which is 79.5% of the cost reduction obtained when full knowledge of the aircraft arrival/departure times is available in advance. We also show that the consideration of stochastic arrival/departure times leads to a higher cost reduction compared to the case when only average point estimates of these times are considered, which achieves an average cost reduction of €10 276 per ETV per day (84.9% of the cost reduction achieved with our proposed approach).

The main contributions of this paper are twofold:

(i) We pose the ETV planning problem as a dynamic Electric Vehicle Routing Problem with Time Windows (E-VRP-TW) that accounts for uncertain aircraft arrival and departure times. This addresses a current research gap in existing studies on ETV planning (Chen et al., 2024), where full knowledge of the aircraft arrival/departure times is assumed.
(ii) We show that considering arrival/departure times as stochastic variables, rather than using point estimates of these times, leads to significant cost reductions: an increase of 17.7%. This emphasizes the importance of planning based on distributions of the arrival/departure times, instead of averages.

The remainder of the paper is organized as follows. Section 2 presents a literature review on which planning models have been developed for (stochastic) electric vehicle scheduling. Section 3 illustrates the uncertainty in flight arrival/departure times. We develop our ETV scheduling framework in Sections 4 and 5, and present two benchmark ETV planning algorithms in Section 6. These are applied in a case study in Sections 7 and 8.

## 2. Prior work and contributions

The planning of ETVs is related to the Vehicle Routing Problem with Time Windows (VRP-TW), where a set of vehicles has to visit a set of customers within their personal time window (Bräysy and Gendreau, 2005a,b). The objective of this is the minimization of the fleet size to visit all customers (Figliozzi, 2010), the travelled distance (Savelsbergh, 1992), or the total transportation costs (Taş, 2021). Here, the main research directions are: VRP-TWs for electric vehicles, VRP-TWs with stochastic input data, and on VRP-TW applications to ETV management, see Table 1.

As electric vehicles become more popular, several VRP-TW variants which account for battery limitations have been developed. This E[lectric]-VRP-TW problem requires vehicles to stop at a charging station before their battery is depleted. First, recharging the battery was assumed to take a fixed amount of time, irrespective of the remaining battery charge. This additional constraint increases the required vehicle fleet size, as shown by Conrad and Figliozzi (2011) and Erdoğan and Miller-Hooks (2012) and the service costs per customer, shown by Omidvar and Tavakkoli-Moghaddam (2012). Subsequent research has been devoted to mitigating this effect. Firstly, a recharge time which is dependent on the state-of-charge was considered in Schneider et al. (2014) and Hiermann et al. (2016). The latter has shown that this decreases transportation costs by 10% with respect to the fixed charging time. Secondly, some studies have proposed scheduling methods where vehicles are allowed partial recharging, such as Desaulniers et al. (2016) and Keskin and Çatay (2016). These studies shows that partial recharging reduces the transportation costs by an additional 5%. Recent studies have improved the realism of the battery recharging process, by introducing batteries for which the recharge rate decreases when they approach full capacity (Zuo et al., 2019; Lam et al., 2022; Diefenbach et al., 2023).

Some elements of the (E-)VRP-TW problem have been carried over to the domain of ETVs. The topic was first introduced without considering battery limitations, similar to the VRP-TW problem, by Soltani et al. (2020). This study performs a cost–benefit analysis of the ETV fleet size. However, charging ETVs has been shown to take a significant amount of time during the day (Lukic et al., 2019), and hence this study overestimates the ETV performance. Baaren and Roling (2019) considered the E-VRP-TW problem for ETVs with constant charging times, as in Conrad and Figliozzi (2011). Lastly, the E-VRP-TW problem with partial charging, as

**Table 1**
Literature on dynamic and/or stochastic (E-)VRP(-TW) problems and applications to ETVs.

| Paper | Vehicles[a] | TW | Uncertainty | Dynamic | Algorithm |
|---|---|---|---|---|---|
| Savelsbergh (1992) | ICE | Yes | – | – | Local search |
| Conrad and Figliozzi (2011) | EV | Yes | – | – | Construction and improvement heuristic |
| Schneider et al. (2014) | EV-soc | Yes | – | – | Variable neighbourhood and tabu search hybrid |
| Hiermann et al. (2016) | EV-soc | Yes | – | – | Large neighbourhood search |
| Desaulniers et al. (2016) | EV-preemp | Yes | – | – | Exact branch price-and-cut |
| Keskin and Çatay (2016) | EV-preemp | Yes | – | – | Large neighbourhood search |
| Soltani et al. (2020) | ICE | Yes | – | – | Branch and bound |
| Baaren and Roling (2019) | EV-fc | Yes | – | – | Branch and bound |
| van Oosterom et al. (2023) | EV-preemp | Yes | – | Yes | Branch and bound |
| Zoutendijk and Mitici (2024) | EV-preemp | Yes | – | – | Adaptive large neighbourhood search |
| Lorini et al. (2011) | ICE | No | Travel times | Yes | Local descent |
| Taş et al. (2014) | ICE | Yes | Travel time | – | Tabu search |
| Pelletier et al. (2019) | EV | No | Energy consumption | No | Adaptive large neighbourhood search |
| Keskin and Çatay (2018) | EV-preemp | Yes | Charge station waiting time | No | Adaptive large neighbourhood search |
| Zhang et al. (2022) | EV | Yes | Energy consumption | No | Robust branch-and-price |
| Messaoud (2023) | EV-preemp | Yes | Travel time | No | Large neighbourhood search |
| Zoutendijk et al. (2023) | EV-preemp | Yes | Time windows | Yes | Branch and bound |

[a] "ICE" = Internal Combustion Engine; "EV" = Electric Vehicles, constant time charging;
"EV-soc" = Electric Vehicles, dynamic charge time; "EV-preemp" = Electric Vehicles, charging preemptively.

in Keskin and Çatay (2016) has been considered for ETVs by van Oosterom et al. (2023). This model was used in a case study at Amsterdam Airport Schiphol to evaluate the minimum required ETV fleet size. It was shown that this approach significantly improves the ETV performance when compared with the non-charging approach in Soltani et al. (2020) and with the fixed charging time approach in Baaren and Roling (2019). Lastly, Zoutendijk and Mitici studied this problem with limits on the number of charging points (Zoutendijk and Mitici, 2024).

To account for uncertainties in the charging and/or operations of electric vehicles, the E-VRP-TW has been expanded to include both *stochastic information* and *dynamic scheduling* (Pillac et al., 2013). *Stochastic information* considers instances where not all parameters of the problem are known with certainty (opposed to deterministic information), but their distributions are known and are taken into account in the models. *Dynamic scheduling* considers instances where parameters of the problem change during the execution of the schedule, and the schedule can be adapted (opposed to static scheduling). Problems can also be both stochastic and dynamic at the same time.

Research on optimizing VRPs under uncertainty started for conventional non-electric vehicles. Lorini et al. (2011) and Taş et al. (2014) studied a VRP where travelling times were uncertain and evolved (due to e.g. traffic jams). The former used the latest travel times to reroute vehicles and reduce travelling time (dynamic planning). Taş et al. (2014) also considered this, but used robust optimization techniques (Bertsimas and Sim, 2004) to account for this uncertainty beforehand (stochastic planning).

In recent years, dynamic and stochastic VRPs have also been studied for electric vehicles. Most studies address battery-related uncertainties, such as energy consumption by Pelletier et al. (2019) and Zhang et al. (2022) or charging time uncertainty by Keskin and Çatay (2018). Only Messaoud (2023) studied the E-VRP-TW under travel time uncertainty, using chance-constrained programming (Charnes and Cooper, 1959). However, this study only considers static planning, and thus ignores that more accurate information becomes available throughout the day.

Zoutendijk et al. (2023) illustrated the possibility of deterministic but dynamic scheduling of ETVs with flight delay uncertainty. It was assumed that the actual arrival/departure time is known 30 min in advance and that the schedule may be updated accordingly. However, this method ignores the fact that flight times are not exactly known in advance, especially when considering departures (as it is shown in the next section). Hence, a realistic ETV scheduling implementation which accounts for flight delays is lacking.

## 3. Stochastic aircraft arrival/departure times

In order to schedule ETVs efficiently, accurate information about the arrival and departure times of flights is required. Though the actual arrival and departure times are unknown, estimates for these are issued. Hours prior to landing, inbound flights are assigned an Estimated Landing Time (ELDT); hours prior to departure, outbound flights are assigned an Estimated Off-Block Time (EOBT, the moment an aircraft leaves the gate). These are updated at subsequent times $t_1, t_2, \dots, t_n$, with $t_1 < t_2 < \cdots t_n$. Let $\text{ELDT}_f(t)$ or $\text{EOBT}_f(t)$ denote the ELDT or EOBT of a flight $f$ at some time $t$, respectively. The actual landing/off-block time of a flight $f$ is denoted as the ALDT or AOBT.

To assess the quality of the EOBT and ELDT, we are interested in the uncertainty of these estimates, i.e., ALDT - ELDT and AOBT - EOBT. Specifically, we consider the distribution of $\text{ALDT}_f$ - $\text{ELDT}_f(t)$ or $\text{AOBT}_f$ - $\text{EOBT}_f(t)$ when there is $\delta$ time remaining before the expected landing/off-block, i.e. when $ELDT_f(t) - t = \delta$ or $EOBT_f(t) - t = \delta$. For example, we consider the distribution of the ALDT - ELDT at the moment when it is expected that $\delta = 120$ min are remaining until the landing of aircraft $f$. Let the random variables $\Delta\text{OBT}_\delta$ and $\Delta\text{LDT}_\delta$ denote the difference AOBT-EOBT and ALDT-ELDT when there is $\delta$ time remaining until the EOBT or ELDT.

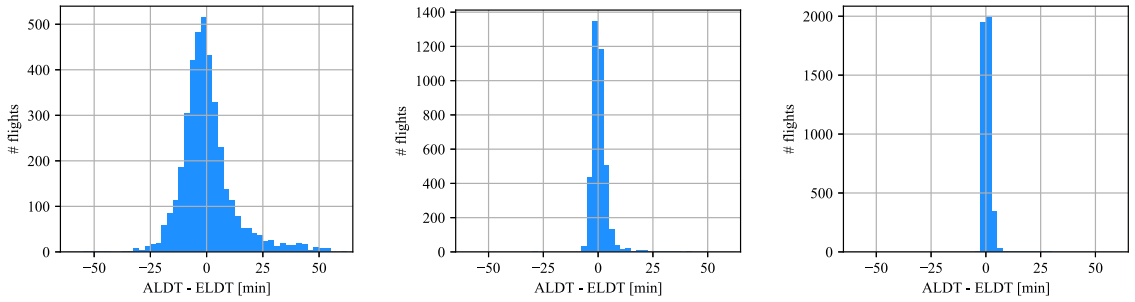


(a) ELDT error when $\delta = 120$ min until expected landing. (b) ELDT error when $\delta = 30$ min until expected landing. (c) ELDT error when $\delta = 5$ min until expected landing.

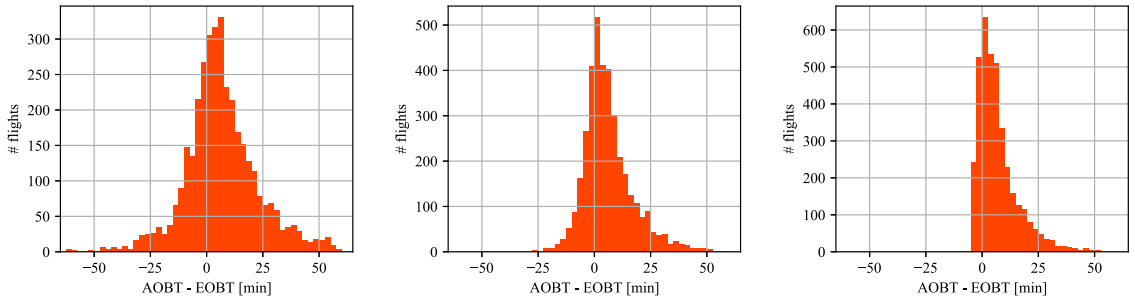


(d) EOBT error when $\delta = 120$ min until expected off-block. (e) EOBT error when $\delta$ =30 min until expected off-block. (f) EOBT error when $\delta = 5$ min until expected off-block.

**Fig. 1.** Histogram of the uncertainty in the ELDT (Figs. 1(a), 1(b), 1(c)) and the EOBT (Figs. 1(d), 1(e), 1(f)) at Amsterdam Schiphol, with $\delta \in \{120, 30, 5\}$ min. Flights of narrow-body aircraft between July 1 - August 30 2023 (74 458 flights) are considered.

Fig. 1 shows the probability density of these variables at $\delta = 120$ min (1(a), 1(d)), 30 min (1(b), 1(e)), and 5 min (1(c), 1(f)) remaining before the estimated landing/off-block, where $\Delta\text{LDT}_\delta$ and $\Delta\text{OBT}_\delta$ are empirically determined based on the flight schedules and actual landing/departure times at Amsterdam Airport Schiphol during July and August 2023. The results show that the uncertainty associated with the EOBT and ELDT, and especially in the case of the ELDT, reduces closer to the actual time of arrival/departure. For our ETV planning, we aim to integrate these random variables within the ETV planning. The ETV plan is reevaluated with every update of the EOBT and ELDT.

## 4. Problem description

We consider the following problem description of an environmentally-aware planning of ETVs taking into account stochastic arrival/departure times. An overview of the used notation can be found in Appendix.

### 4.1. ETV model and towing process

Let $V$ denote the set of ETVs. Each ETV is equipped with a battery with energy capacity $E$. Fig. 2 illustrates the process of towing an aircraft using an ETV (van Oosterom et al., 2023). A departing aircraft is first connected to an ETV, which performs the push-back. The push-back starts at the AOBT (Actual Off-Block Time, Section 3). After that, the aircraft is towed to the runway and the ETV is disconnected at a holding point. Without the ETV, the aircraft warms up its engines, taxis onto the runway and takes off. An arriving aircraft follows the same steps in reverse order, and without a push-back phase. We aim to have an ETV at the aircraft as soon as the aircraft' engines have cooled down, at $\Delta t^{\text{ec}}$ after the ALDT (Actual Landing Time).

The following is assumed:

- **(A1)** ETVs tow aircraft at a constant velocity $v^x$ and drive (while not towing) at a velocity $v^s$.
- **(A2)** The energy used per unit distance, $\mathcal{E}(v, m)$, depends on the driving velocity $v$ and towed mass $m$.
- **(A3)** For the ETV battery charging process, we assume a bi-linear charging profile (see Fig. 3) with parameters $\alpha, \beta \in (0, 1)$ (Mitici et al., 2022). Up to $\alpha E$, the battery is recharged with power $P^c$. From $\alpha E$ up to $E$, the battery recharges with power $\beta P^c$.
- **(A4)** An ETV battery should be recharged for at least $\Delta t^c_{\text{min}}$ time.
- **(A5)** An ETV starts and ends the day of operations with a fully charged battery.

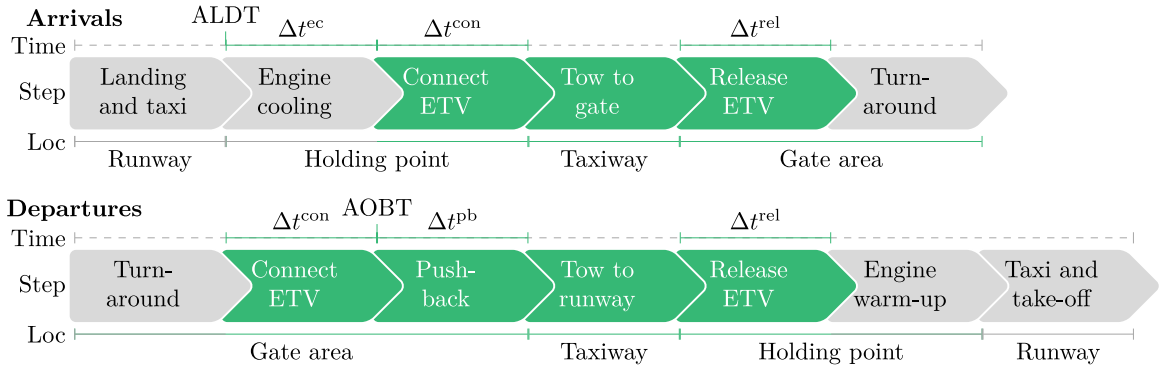


**Fig. 2.** Towing process for departing/arriving aircraft. An ETV is connected to an aircraft in the green time blocks (van Oosterom et al., 2023).

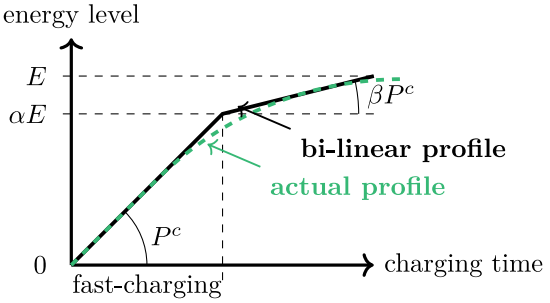


**Fig. 3.** Bilinear and actual charging profile. The battery energy level is given as a function of the charging time (van Oosterom et al., 2023).

### 4.2. Airport taxiway and service roads

We consider an airport represented by a directed graph $G = (N, A)$. The set of nodes $N$ contains the runway holding points and gates $N^{rg} \subset N$ and ETV charging stations $N^c \subset N$. One of the charging locations is also the depot of the ETVs, $n^{dep} \in N^c$. Let $l : A \to \mathbb{R}_+$ denote the lengths of the arcs of graph $G$. Arcs are either a taxiway $A^X \subset A$ or a service road $A^S \subset A$.

- **(A6)** When towing an aircraft between gates and runways, ETVs use the shortest path using only arcs of the taxiway network $A^X$. The length of this shortest path is given by $d^X : N \times N \to \mathbb{R}_+$.
- **(A7)** When not towing an aircraft, ETVs traverse the airport using the shortest path given the service road arcs $A^S$. The length of this path is given by $d^S : N \times N \to \mathbb{R}_+$.
- **(A8)** ETVs always start and end their day at the depot $n^{dep} \in N^c$.

### 4.3. Arriving/departing aircraft

We consider a period of time $T = [t_s, t_e]$, representing a day of operations starting at $t_s$ and ending at $t_e$. During $T$, a set $F$ of aircraft arrive to and depart from the airport which can be towed by ETVs. Let $F^{arr} \subset F$ and $F^{dep} \subset F$ denote the set of arriving and departing aircraft, respectively. Each $f \in F$ is defined by a tuple $(n_f^{\mathrm{p}}, n_f^{\mathrm{d}}, m_f, c_f^{\mathrm{taxi}}, c_f^{\mathrm{tow}}, \tau_f^{\mathrm{p}})$, where $n_f^{\mathrm{p}} \in N^{rg}$ and $n_f^{\mathrm{d}} \in N^{rg}$ denote the locations where the aircraft should be picked up and dropped off by an ETV, and $m_f$ denotes the mass of aircraft $f$. When no ETV is available to tow $f$, it must taxi by itself. A cost $c_f^{\mathrm{taxi}}$ is incurred when $f$ taxis, due to fuel consumption and emissions. Towing $f$ costs $c_f^{\mathrm{tow}}$, related to the electricity consumed (where $c_f^{\mathrm{tow}} < c_f^{\mathrm{taxi}}$).

At a given time $t \in T$, with $\delta = EOBT_f(t) - t$ expected remaining time until off-block (or $\delta = ELDT_f(t) - t$ until landing), let $\tau_f^{\mathrm{p}}(t)$ denote the pick-up time of aircraft $f$, where:

$$\tau_f^{\mathrm{p}}(t) = \begin{cases} \Delta\mathrm{OBT}_\delta + EOBT_f(t) - \Delta t^{\mathrm{con}} & \text{if } f \in F^{dep}, \\ \Delta\mathrm{LDT}_\delta + ELDT_f(t) + \Delta t^{\mathrm{ec}} & \text{if } f \in F^{arr}, \end{cases} \tag{1}$$

where, $\tau_f^{\mathrm{p}}(t)$ is a stochastic variable since we do not know the AOBT/ALDT beforehand.

From $\tau_f^{\mathrm{p}}(t)$, the drop-off time of aircraft $f$ is defined as:

$$\tau_f^{\mathrm{d}}(t) = \tau_f^{\mathrm{p}}(t) + \Delta t^{\mathrm{con}} + \mathbf{1}_{\{f \in F^{dep}\}} \Delta t^{\mathrm{pb}} + d^X(n_f^{\mathrm{p}}, n_f^{\mathrm{d}})/v_x + \Delta t^{\mathrm{rel}}, \tag{2}$$

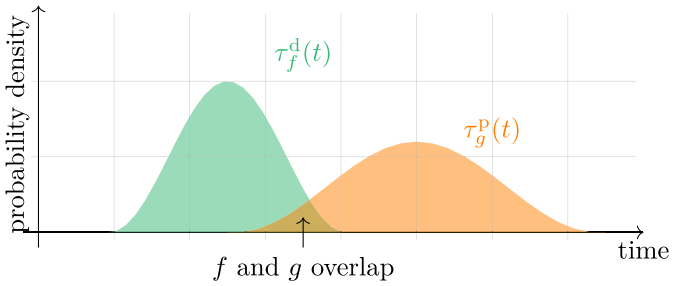


**Fig. 4.** Example of the pick-up time and drop-off time random variables of flights $f$ and $g$, with $n_g^{\mathrm{p}} = n_f^{\mathrm{d}}$. With probability $\mathbb{P}[\tau_{fg}^{\mathrm{o}}(t) > 0]$, the two aircraft cannot be towed with the same ETV.

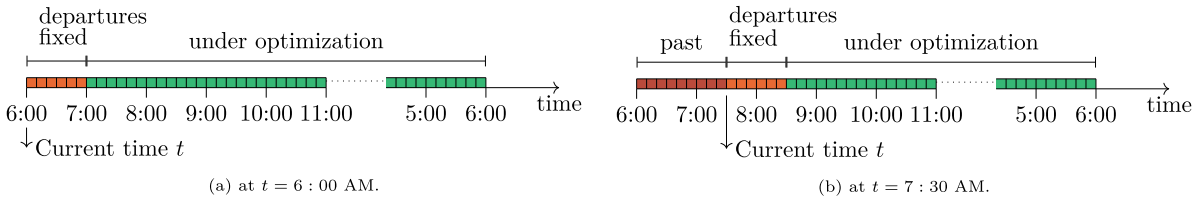


**Fig. 5.** Illustration of two ETV planning reevaluation moments with $T$ starting and ending at 6 AM and $\Delta t^{fix} = 1$ h.

which is the first moment an ETV is disconnected after it has towed $f$ and is available to proceed to its next task. Lastly, we define the overlap time $\tau_{fg}^{\mathrm{o}}$ as the time by which an ETV is early or too late to tow $g$, if $g$ is towed subsequently after $f$. It is given by:

$$\tau_{fg}^{\mathrm{o}}(t) = \tau_g^{\mathrm{p}}(t) - \left(\tau_f^{\mathrm{d}}(t) + d^s(n_f^{\mathrm{d}}, n_g^{\mathrm{p}})/v_s\right) \tag{3}$$

Fig. 4 shows an example of the pick-up/drop-off random variables for two flights $f$ and $g$: $\tau_f^{\mathrm{d}}(t)$ and $\tau_g^{\mathrm{p}}(t)$. Assume that $n_f^{\mathrm{d}} = n_g^{\mathrm{p}}$, such that an ETV can pick-up $g$ immediately after dropping-off $f$. Note that the two random variables overlap, i.e. $\mathbb{P}[\tau_{fg}^{\mathrm{o}}(t) > 0] > 0$, such that there is a non-zero probability that the tow of flight $g$ starts before the end of the tow of flight $f$, thus one single ETV may not be able to tow both flights.

We assume:

**(A9)** For $f \in F^{arr}$ to be towed, an ETV needs to be present at $n_f^{\mathrm{p}}$ by $ALDT_f + \Delta t^{\mathrm{ec}}$ (see Fig. 2).

**(A10)** If $f \in F^{dep}$ is towed, a monetary cost $c_f^{\mathrm{d}}$ is incurred for every unit of time an ETV is not present at $n_f^{\mathrm{p}}$ after the desired pick-up time $AOBT_f - \Delta t^{\mathrm{con}}$ (see Fig. 2).

### 4.4. Dynamically updating the ETV planning

As $\tau_f^{\mathrm{p}}(t)$ is updated based on the updated ELDT or EOBT, the planning of the ETVs is reevaluated. Flights may be assigned to and unassigned from ETVs, and the ETV battery recharging times may change. This is allowed at any time $t \in T$. For this, we make the following assumptions:

**(A11)** An arriving aircraft may be assigned to or unassigned from an ETV at any moment before the pick-up time.

**(A12)** Up to a period $\Delta t^{fix}$ from the current time $t$, the assignment of departing aircraft $f$ to ETVs is fixed (while $\mathbb{E}[\tau_f^{\mathrm{p}}(t)] < t + \Delta t^{fix}$). After that, the assignment of $f$ can be changed.

Before the current time $t$, the ETV planning is fixed. Between $t$ and $t + \Delta t^{fix}$, the ETV planning may be altered, but only arriving aircraft may be assigned or unassigned from an ETV. This is proposed in order to conform with assumption **(A9)**. In order to avoid a schedule which is too erratic in the near future, which would be difficult to be implemented by operators, the schedule for departing aircraft is fixed. After $t + \Delta t^{fix}$, the ETV schedule may be altered for both arriving and departing aircraft. Fig. 5 shows how the ETV planning may be dynamically updated. Fig. 5(a) shows the situation at $t = 6$ AM, and Fig. 5(b) at $t = 7$ AM.

### 4.5. ETV scheduling objective

When no ETV tows an aircraft $f$, it taxis by itself. The resulting emissions lead to an (environmental) cost $c_f^{\mathrm{taxi}} - c_f^{\mathrm{tow}}$ per aircraft, which is a function of the aircraft type and taxi distance. Also, when departing aircraft are delayed because no ETV is available to tow them to the runway, a cost $c_f^{\mathrm{d}}$ per delayed aircraft is incurred per unit of time **(A10)**.

Given (i) a fleet of ETVs $V$, (ii) the airport layout $(N, A)$, and (iii) the set of arriving/departing aircraft $F$, we aim to determine an environmentally-aware, dynamic ETV planning. This planning is conform all mentioned assumptions, and can be reevaluated at

any time during the day. The objective is to minimize the total cost associated with (a) the cost of taxiing emissions $c^{\text{taxi}} - c^{\text{tow}}$ due to ETVs not being available to tow aircraft, i.e. those aircraft that are taxiing by themselves, and (b) the cost $c^{\text{d}}$ associated with departure delays caused by towing.

## 5. Stochastic pick-up time for ETV planning

In this section we propose a rolling horizon algorithm to plan operations for a fleet of ETVs that considers uncertain aircraft arrival and departure times. An overview of the used notation can be found in Appendix.

At each moment, an ETV $v$ is described by its state. This is given by a tuple $(n_v, t_v, E_v, F_v, S_v)$, which gives the current location, time, battery energy level, flights to tow, and the current activity, respectively. There are four possible ETV activities for $S_v$: tow, drive, charge, or idle. An ETV can be idle if it is waiting to tow an aircraft or when its battery is full and $F_v = \emptyset$.

Algorithm 1 shows the framework of our approach. The ETV state is initialized at the start of the day. The algorithm uses two subroutines which update the state of the ETVs. The first subroutine is a MILP that optimizes the ETV planning for the rest of the day (Section 5.1) while anticipating delays. The second is a greedy algorithm that performs the planning and resolves conflicts when delays occur (Section 5.2). Fig. 5 shows two epochs of the rolling horizon algorithm, using $\Delta t^{fix} = 1$ h.

**Algorithm 1:** Dynamic ETV planning framework.

**Data:** Airport layout, Day of operations $T = [t_s, t_e]$, fleet of ETVs $V$, set of flights $F$, $\Delta t^{fix}$, $\Delta t^{reopt}$, $\delta t$.
**Result:** Dynamic ETV schedule

```
Initialize current time t = t_s − Δt^fix;
Initialize ETV states: n_v = n^dep, t_v = t, E_v = E, F_v = {}, S_v = idle;
while t < t_e do
    Globally reevaluate the ETV schedule (Section 5.1) and update F_v for all ETVs;
    Set t' ← t + Δt^reopt ;
    while t ≤ t' do
        for v ∈ V if t_v ≤ t do
            Run ExecuteTows (Section 5.2) to obtain the new ETV state (n'_v, t'_v, E'_v, F'_v, S'_v);
            Set (n_v, t_v, E_v, F_v, S_v) ← (n'_v, t'_v, E'_v, F'_v, S'_v) ;
        end
        Set t ← t + δt;
        Update the flight EOBT and ELDT information;
    end
end
```

### 5.1. Global ETV planning

At any given time $t$ during the day of operations $T$, we aim to optimize the planning of the ETVs for the remainder of the day of operations. We aim for a robust planning, anticipating the uncertainty in the pick-up times of the aircraft, the varying demand for ETVs across the day, and the need to recharge the ETV batteries. This optimization generates a list of to-be-towed flights $F_v$ for all ETVs.

We optimize the schedule for the period after $t$. Each ETV finishes the task it is performing at $t$, and is available for reassignment after this moment. Vehicle $v \in V$ is then located at node $n_v^{\text{a}}$ at time $\tau_v^{\text{a}}$ with battery charge $E_v$. We define the following sets (see Fig. 6):

- Let $F^{fix}$ be the set of departures $f$ which were previously assigned to an ETV and have $EOBT_f(t) < t + \Delta t^{reopt}$.
- Let $F'$ be the set of flights which can still be towed by the ETVs. These are the flights which can be reached on time by at least one of the ETVs in $V$, given their first availability $(n_v^{\text{a}}, \tau_v^{\text{a}}, E_v)$, with probability at least $\mathbb{P}_\phi$:

$$F' := \{f \in F : \exists v \in V : \mathbb{P}[\tau_f^{\text{p}} \geq \tau_v^{\text{a}} + d^s(n_v^{\text{d}}, n_f^{\text{p}})/v_s] \geq \mathbb{P}_\phi\} \setminus \{f \in F^{dep} : \mathbb{E}[\tau_f^{\text{p}}(t)] < t + \Delta t^{fix}\}.$$

  The set $F'$ also includes an artificial flight $f^{end}$ with $n_{f^{end}}^{\text{p}} = n_{f^{end}}^{\text{d}} = n^{dep}$, $\tau_{f^{end}}^{\text{p}} = t_e$, and which requires charge $E$. This flight will be used in the MILP formulation (Section 5.1.3).
- Let $V_f \subset V$ be the ETVs which are able to tow flight $f \in F'$, given their first availability $(n_v^{\text{a}}, \tau_v^{\text{a}}, E_v)$.
- Let $F'_f \subset F'$ be the flights which can be towed before $f$ by the same ETV.

In between towing two aircraft $f$ and $g$, an ETV may have the opportunity to recharge its battery at a charging station in $N^c$. ETVs use the station which requires the shortest detour between the drop-off point of $f$ and the pick-up point of $g$, which is denoted by $n_{fg}^c$. For simplicity, we introduce the following abbreviations:

$$E^X(f) := \mathcal{E}(m_f, v^x) \cdot d^X(n_f^{\text{p}}, n_f^{\text{d}}) \qquad f \in F', \tag{4a}$$

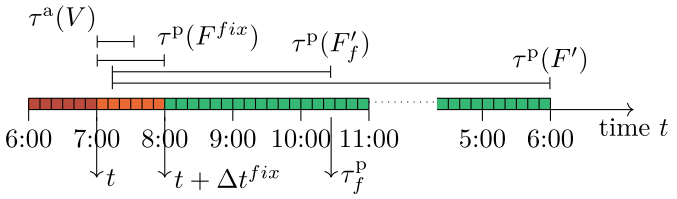


**Fig. 6.** Expected pick-up times of flights $F'$ and $F'_f$ for a flight $f \in F'$, denoted by $\tau^{\mathrm{p}}(F')$ and $\tau^{\mathrm{p}}(F'_f)$ respectively, together with the first availability times of the ETVs in $V$, denoted by $\tau^{\mathrm{a}}(V)$. The current time is $t = 7$ AM, and $\Delta t^{fix} = 1$ h.

$$E^S(f,g) := \mathcal{E}(0,v^s) \cdot \begin{cases} d^S(n^{\mathrm{d}}_f, n^{\mathrm{p}}_g) & f \in F'_g \\ d^S(n^{\mathrm{a}}_f, n^{\mathrm{p}}_g) & f \in V_g \end{cases} \qquad g \in F', \tag{4b}$$

$$E^S_l(f) := \mathcal{E}(0,v^s) \cdot \begin{cases} d^S(n^{\mathrm{d}}_f, n^{dep}), \\ d^S(n^{\mathrm{a}}_f, n^{dep}), \end{cases} \qquad \begin{matrix} f \in F', \\ f \in V, \end{matrix} \tag{4c}$$

$$E^S_c(f,g) := \mathcal{E}(0,v^s) \cdot \begin{cases} \left(d^S(n^{\mathrm{d}}_f, n^c_{fg}) + d^S(n^c_{fg}, n^{\mathrm{p}}_g)\right) & f \in F'_g \\ \left(d^S(n^{\mathrm{a}}_f, n^c_{fg}) + d^S(n^c_{fg}, n^{\mathrm{p}}_g)\right) & f \in V_g \end{cases} \qquad g \in F', \tag{4d}$$

$$E^S_{c1}(f) := \mathcal{E}(0,v^s) \cdot \begin{cases} \max_{n^c \in N^c} d^S(n^{\mathrm{d}}_f, n^c) \\ \max_{n^c \in N^c} d^S(n^{\mathrm{a}}_f, n^c) \end{cases} \qquad \begin{matrix} f \in F', \\ f \in V. \end{matrix} \tag{4e}$$

Here, $E^X(f)$ denotes the energy required to tow aircraft $f$, $E^S(g,f)$ the energy required to drive directly from the drop-off of $f$ to the pick-up of aircraft $g$, and $E^S_l(f)$ the energy required to drive from the drop-off of $f$ to the depot. The energy required to drive from the drop-off of $g$ to the pick-up of $f$ via the charging station $n^c_g$ is given by $E^S_c(g,f)$. It is assumed that ETVs use the shortest path in the network **(A2)**.

For an aircraft $f \in F'$ and an aircraft $g \in F'_f$ or ETV $v \in V_f$, we denote the available charging time before towing $f$ as $\Delta t^c(g,f)$ and $\Delta t^c(v,f)$, which are both random variables, respectively. We allow an ETV to recharge if this time is longer than $\Delta t^c_{\min}$ with probability at least $\mathbb{P}_\theta$ **(A4)**. The sets of all aircraft and ETV departure points for which this holds are denoted by:

$$F'^c_f := \{g \in F'_f : \mathbb{P}[\Delta t^c(g,f) \geq \Delta t^c_{\min}] \geq \mathbb{P}_\theta\}, \qquad V^c_f := \{v \in V_f : \mathbb{P}[\Delta t^c(v,f) \geq \Delta t^c_{\min}] \geq \mathbb{P}_\theta\} \tag{5}$$

### 5.1.1. Decision variables

We consider the following indicator decision variables, which determine which aircraft are towed by each of the ETVs:

$$x_{fg} \in \{0,1\}, \qquad \text{with } g \in F', f \in F'_g \cup V_g, \tag{6a}$$

If $f \in V_g$ and $x_{fg} = 1$, aircraft $g$ is the first towed aircraft by $f$ after $t$. If $f \in F'_g$ and $x_{fg} = 1$, aircraft $f$ and $g$ are towed consecutively by the same ETV **(A11)** and **(A12)**. Different from previous ETV planning studies (Soltani et al., 2020; Zoutendijk and Mitici, 2024), we do not require the decision variable $x$ to keep track of the specific ETV, i.e. we do not define a decision variable $x_{fgv}$ for each ETV $v \in V$. This significantly reduces the size of the MILP model.

We also define the variable $E_f$ which tracks the battery energy level of the ETV batteries, i.e.,

$$E_f \in \mathbb{R}_+, \qquad \text{ETV battery energy level at the start of towing flight } f \tag{6b}$$

### 5.1.2. Objective function

We use the information about the uncertainty in the pick-up times to define the objective function. When no aircraft is towed, a total (environmental) cost $\sum_{f \in F'} c^{\mathrm{taxi}}_f$ is incurred, which consists of the costs related to fuel consumption and emissions during taxiing. This cost is reduced by towing flights, and we aim to maximize this cost reduction. When ignoring delays, this reduction is given by:

$$\sum_{g \in F'} \left[ \left(c^{\mathrm{taxi}}_g - c^{\mathrm{tow}}_g\right) \sum_{f \in F'_g \cup V_g} x_{fg} \right] = \sum_{g \in F'} \sum_{f \in F'_g \cup V_g} \tfrac{1}{2} \left(c^{\mathrm{taxi}}_f - c^{\mathrm{tow}}_f + c^{\mathrm{taxi}}_g - c^{\mathrm{tow}}_g\right) x_{fg} := \sum_{g \in F'} \sum_{f \in F'_g \cup V_g} c_{fg}(0) x_{fg},$$

where $c_{fg}(\cdot)$ denotes the cost reduction achieved when $x_{fg} = 1$, i.e., when flight $f$ is towed immediately after flight $g$ by the same ETV. This coefficient is a function of the overlap time (defined in Section 4.3): $c_{fg}(\tau^{\mathrm{o}})$. When $\tau^{\mathrm{o}} > 0$, $g$ may have to be delayed, or

one of the aircraft is not towed at all (thus it has to taxi on its own). We aim to maximize the expected cost reduction:

$$\max_{x,q} \sum_{g \in F'} \sum_{f \in F'_g \cup V_g} \mathbb{E}[c_{fg}(\tau^{\mathrm{o}}_{fg}(t))] x_{fg}. \tag{7a}$$

As different assumptions are made for planning in- and outbound aircraft (Section 4.4), $\mathbb{E}[c_{fg}(\tau^{\mathrm{o}}_{fg}(t))]$ has to be determined for all six possible cases when $f$ is an ETV or in/outbound aircraft and $g$ is an in/outbound aircraft as follows:

- Case 1: $f$ **departure,** $g$ **departure:** Both $f$ and $g$ have to be towed if they are assigned to ETVs (A12). If the overlap time is positive, aircraft $g$ needs to wait for the ETV to arrive. As such, we incur a delay cost $\tau^{\mathrm{o}} c^{\mathrm{d}}_g$. With this, we have:

$$c_{fg}(\tau^{\mathrm{o}}) = \tfrac{1}{2}\left(c^{\mathrm{taxi}}_f - c^{\mathrm{tow}}_f + c^{\mathrm{taxi}}_g - c^{\mathrm{tow}}_g\right) - c^{\mathrm{d}}_g \times \max\{\tau^{\mathrm{o}}, 0\},$$

  which has the expected value:

$$\begin{aligned}
\mathbb{E}[c_{fg}(\tau^{\mathrm{o}}_{fg}(t))] &= \mathbb{E}\left[\tfrac{1}{2}\left(c^{\mathrm{taxi}}_f - c^{\mathrm{tow}}_f + c^{\mathrm{taxi}}_g - c^{\mathrm{tow}}_g\right) - c^{\mathrm{d}}_g \times \max\{\tau^{\mathrm{o}}_{fg}(t), 0\}\right] \\
&= \tfrac{1}{2}\left(c^{\mathrm{taxi}}_f - c^{\mathrm{tow}}_f + c^{\mathrm{taxi}}_g - c^{\mathrm{tow}}_g\right) - \mathbb{E}\left[\max\{\tau^{\mathrm{o}}_{fg}(t), 0\}\right] \times c^{\mathrm{d}}_g \\
&= \tfrac{1}{2}\left(c^{\mathrm{taxi}}_f - c^{\mathrm{tow}}_f + c^{\mathrm{taxi}}_g - c^{\mathrm{tow}}_g\right) - \mathbb{P}[\tau^{\mathrm{o}}_{fg}(t) > 0] \times \mathbb{E}[\tau^{\mathrm{o}}_{fg}(t) | \tau^{\mathrm{o}}_{fg}(t) > 0] \times c^{\mathrm{d}}_g
\end{aligned} \tag{7b}$$

- Case 2: $f$ **departure,** $g$ **arrival:** Aircraft $g$ can be either towed by an ETV or it can taxi by itself (A11), whereas $f$ needs to be towed (A12). Aircraft $g$ is not towed if there is overlap. In this case, we have:

$$c_{fg}(\tau^{\mathrm{o}}) = \tfrac{1}{2}(c^{\mathrm{taxi}}_f - c^{\mathrm{tow}}_f) + \tfrac{1}{2}(c^{\mathrm{tow}}_g - c^{\mathrm{taxi}}_g) \qquad \text{if} \qquad \tau^{\mathrm{o}} > 0,$$

  which gives:

$$\begin{aligned}
\mathbb{E}[c_{fg}(\tau^{\mathrm{o}}_{fg}(t))] &= \mathbb{P}[\tau^{\mathrm{o}}_{fg}(t) \le 0] \times \mathbb{E}[c_{fg}(\tau^{\mathrm{o}}_{fg}) | \tau^{\mathrm{o}}_{fg}(t) \le 0] + \mathbb{P}[\tau^{\mathrm{o}}_{fg}(t) > 0] \times \mathbb{E}[c_{fg}(\tau^{\mathrm{o}}_{fg}) | \tau^{\mathrm{o}}_{fg}(t) > 0] \\
&= \mathbb{P}[\tau^{\mathrm{o}}_{fg}(t) \le 0] \times \tfrac{1}{2}\left(c^{\mathrm{taxi}}_f - c^{\mathrm{tow}}_f + c^{\mathrm{taxi}}_g - c^{\mathrm{tow}}_g\right) + \mathbb{P}[\tau^{\mathrm{o}}_{fg}(t) > 0] \times \tfrac{1}{2}\left(c^{\mathrm{taxi}}_f - c^{\mathrm{tow}}_f - c^{\mathrm{taxi}}_g + c^{\mathrm{tow}}_g\right) \\
&= \tfrac{1}{2}(c^{\mathrm{taxi}}_f - c^{\mathrm{tow}}_f) + \tfrac{1}{2}(c^{\mathrm{taxi}}_g - c^{\mathrm{tow}}_g)\mathbb{P}[\tau^{\mathrm{o}}_{fg}(t) \le 0] - \tfrac{1}{2}(c^{\mathrm{taxi}}_g - c^{\mathrm{tow}}_g)\mathbb{P}[\tau^{\mathrm{o}}_{fg}(t) > 0] \\
&= \tfrac{1}{2}\left(c^{\mathrm{taxi}}_f - c^{\mathrm{tow}}_f + c^{\mathrm{taxi}}_g - c^{\mathrm{tow}}_g\right) - \mathbb{P}[\tau^{\mathrm{o}}_{fg}(t) > 0] \times (c^{\mathrm{taxi}}_g - c^{\mathrm{tow}}_g)
\end{aligned} \tag{7c}$$

- Case 3: $f$ **arrival,** $g$ **arrival:** Both $f$ and $g$ can either be towed by an ETV or taxi by itself when $\tau^{\mathrm{o}} > 0$ (A11). We maximize the reduction in emission cost due to switching to electric towing from conventional taxi. As such, when there is overlap, we choose to tow the aircraft with the highest reduction in emission cost, i.e. the highest $c^{\mathrm{taxi}} - c^{\mathrm{tow}}$. Similar to the previous case, we have:

$$c_{fg}(\tau^{\mathrm{o}}) = \tfrac{1}{2} \max_{h=f,g}\{c^{\mathrm{taxi}}_h - c^{\mathrm{tow}}_h\} + \tfrac{1}{2} \max_{h=f,g}\{c^{\mathrm{tow}}_h - c^{\mathrm{taxi}}_h\} \qquad \text{if} \qquad \tau^{\mathrm{o}} > 0$$

  such that we obtain:

$$\begin{aligned}
\mathbb{E}[c_{fg}(\tau^{\mathrm{o}}_{fg}(t))] &= \mathbb{P}[\tau^{\mathrm{o}}_{fg}(t) \le 0] \times \mathbb{E}[c_{fg}(\tau^{\mathrm{o}}_{fg}) | \tau^{\mathrm{o}}_{fg}(t) \le 0] + \mathbb{P}[\tau^{\mathrm{o}}_{fg}(t) > 0] \times \mathbb{E}[c_{fg}(\tau^{\mathrm{o}}_{fg}) | \tau^{\mathrm{o}}_{fg}(t) > 0] \\
&= \mathbb{P}[\tau^{\mathrm{o}}_{fg}(t) \le 0] \times \tfrac{1}{2}\left(c^{\mathrm{taxi}}_f - c^{\mathrm{tow}}_f + c^{\mathrm{taxi}}_g - c^{\mathrm{tow}}_g\right) \\
&\quad + \mathbb{P}[\tau^{\mathrm{o}}_{fg}(t) > 0] \times \tfrac{1}{2}\left(\max_{h=f,g}\{c^{\mathrm{taxi}}_h - c^{\mathrm{tow}}_h\} + \max_{h=f,g}\{c^{\mathrm{tow}}_h - c^{\mathrm{taxi}}_h\}\right) \\
&= (1 - \mathbb{P}[\tau^{\mathrm{o}}_{fg}(t) > 0]) \times \tfrac{1}{2}\left(\max_{h=f,g}\{c^{\mathrm{taxi}}_h - c^{\mathrm{tow}}_h\} + \min_{h=f,g}\{c^{\mathrm{taxi}}_h - c^{\mathrm{tow}}_h\}\right) \\
&\quad + \mathbb{P}[\tau^{\mathrm{o}}_{fg}(t) > 0] \times \tfrac{1}{2}\left(\max_{h=f,g}\{c^{\mathrm{taxi}}_h - c^{\mathrm{tow}}_h\} - \min_{h=f,g}\{c^{\mathrm{taxi}}_h - c^{\mathrm{tow}}_h\}\right) \\
&= \tfrac{1}{2}\left(c^{\mathrm{taxi}}_f - c^{\mathrm{tow}}_f + c^{\mathrm{taxi}}_g - c^{\mathrm{tow}}_g\right) - \mathbb{P}[\tau^{\mathrm{o}}_{fg}(t) > 0] \min_{h=f,g}\left(c^{\mathrm{taxi}}_h - c^{\mathrm{tow}}_h\right)
\end{aligned} \tag{7d}$$

- Case 4: $f$ **arrival,** $g$ **departure:** When there is an overlap, $g$ must be towed (A12). If the overlap time is small enough that the costs of delaying $g$ are less then the cost of letting $f$ taxi by itself, we delay $g$ and tow both $f$ and $g$. In this case, we have:

$$c_{fg}(\tau^{\mathrm{o}}) = \tfrac{1}{2}\left(c^{\mathrm{taxi}}_f - c^{\mathrm{tow}}_f + c^{\mathrm{taxi}}_g - c^{\mathrm{tow}}_g\right) - \tau^{\mathrm{o}} \times c^{\mathrm{d}}_g \qquad \text{if} \qquad 0 \le c^{\mathrm{d}}_g \times \tau^{\mathrm{o}} \le c^{\mathrm{taxi}}_f - c^{\mathrm{tow}}_f.$$

  If the overlap time is larger, when $c^{\mathrm{d}}_g \tau^{\mathrm{o}}_{fg} > c^{\mathrm{taxi}}_f - c^{\mathrm{tow}}_f$, we only tow $g$ (without delay) and let $f$ taxi by itself. In this case, we have:

$$c_{fg}(\tau^{\mathrm{o}}) = \tfrac{1}{2}(c^{\mathrm{tow}}_f - c^{\mathrm{taxi}}_f) + \tfrac{1}{2}(c^{\mathrm{taxi}}_g - c^{\mathrm{tow}}_g) \qquad \text{if} \qquad c^{\mathrm{d}}_g \tau^{\mathrm{o}} > c^{\mathrm{taxi}}_f - c^{\mathrm{tow}}_f.$$

  Combining the three cases, we get:

$$\mathbb{E}[c_{fg}(\tau^{\mathrm{o}}_{fg}(t))] = \mathbb{P}[\tau^{\mathrm{o}}_{fg}(t) \le 0] \times \mathbb{E}[c_{fg}(\tau^{\mathrm{o}}_{fg}) | \tau^{\mathrm{o}}_{fg}(t) \le 0]$$

$$
\begin{aligned}
&+\mathbb{P}[0<\tau^{o}_{fg}c^{d}_{g}\le c^{taxi}_{f}-c^{tow}_{f}]\times\mathbb{E}[c_{fg}(\tau^{o}_{fg})|0<\tau^{o}_{fg}c^{d}_{g}\le c^{taxi}_{f}-c^{tow}_{f}]\\
&+\mathbb{P}[\tau^{o}_{fg}c^{d}_{g}\ge c^{taxi}_{f}-c^{tow}_{f}]\times\mathbb{E}[c_{fg}(\tau^{o}_{fg})|\tau^{o}_{fg}c^{d}_{g}\ge c^{taxi}_{f}-c^{tow}_{f}]\\
=\;&\mathbb{P}[\tau^{o}_{fg}(t)\le 0]\times\tfrac{1}{2}\left(c^{taxi}_{f}-c^{tow}_{f}+c^{taxi}_{g}-c^{tow}_{g}\right)\\
&+\mathbb{P}[0<\tau^{o}_{fg}c^{d}_{g}\le c^{taxi}_{f}-c^{tow}_{f}]\\
&\quad\times\left(\tfrac{1}{2}\left(c^{taxi}_{f}-c^{tow}_{f}+c^{taxi}_{g}-c^{tow}_{g}\right)-c^{d}_{g}\times\mathbb{E}[\tau^{o}_{fg}|0<\tau^{o}_{fg}c^{d}_{g}\le c^{taxi}_{f}-c^{tow}_{f}]\right)\\
&+\mathbb{P}[\tau^{o}_{fg}c^{d}_{g}\ge c^{taxi}_{f}-c^{tow}_{f}]\times\left(\tfrac{1}{2}(c^{tow}_{f}-c^{taxi}_{f})+\tfrac{1}{2}(c^{taxi}_{g}-c^{tow}_{g})\right)\\
=\;&\tfrac{1}{2}\left(c^{taxi}_{f}-c^{tow}_{f}+c^{taxi}_{g}-c^{tow}_{g}\right)\\
&-\mathbb{E}[\tau^{o}_{fg}|0<\tau^{o}_{fg}c^{d}_{g}\le c^{taxi}_{f}-c^{tow}_{f}]\times\mathbb{P}[0<\tau^{o}_{fg}c^{d}_{g}\le c^{taxi}_{f}-c^{tow}_{f}]\\
&-(c^{taxi}_{f}-c^{tow}_{f})\times\mathbb{P}[\tau^{o}_{fg}c^{d}_{g}\ge c^{taxi}_{f}-c^{tow}_{f}]
\end{aligned}
\tag{7e}
$$

- Case 5: $f$ **ETV,** $g$ **arrival**: In the case that $f$ is an ETV, the computation depends on its state. The value $\tau^{o}_{fg}$ is computed using a modified Eq. (3):

$$\tau^{o}_{fg}(t)=\tau^{p}_{g}(t)-(\tau^{a}_{f}+d^{S}(n^{a}_{f},n^{p}_{g})/v_{s}).$$

  In this case, the computations will be the same as in Case 1.
- Case 6: $f$ **ETV,** $g$ **departure:** The value of $\tau^{o}_{fg}(t)$ is computed, and the case is reduced to case 2.

### 5.1.3. MILP model

We use the following MILP formulation, which aims to minimize the expected environmental and delay costs for the remainder of the day (after $t$):

$$\max \quad \sum_{g\in F'}\sum_{f\in F'_g\cup V_g}\mathbb{E}[c_{fg}(\tau^{o}_{fg}(t))]x_{fg} \tag{8a}$$

$$\text{s.t.} \quad 1\ge\sum_{f\in F':v\in V_f}x_{vf} \qquad \forall v\in V, \tag{8b}$$

$$1\ge\sum_{g\in F'_f\cup V_f}x_{gf}=\sum_{g\in F':f\in F'_g}x_{fg}\ge\mathbf{1}_{\{f\in F^{fix}\}} \qquad \forall f\in F'\setminus\{f^{end}\}, \tag{8c}$$

$$E_g\le E_f+E\cdot(1-x_{fg})-x_{fg}\cdot\begin{cases}E^{X}(f)+E^{S}(f,g) & \text{if } f\notin F'^{c}_{g}\cup V^{c}_{g}\\ E^{X}(f)+E^{S}_{c}(f,g)-P^{c}\Delta t^{c}(f,g) & \text{if } f\in F'^{c}_{g}\cup V^{c}_{g}\end{cases} \qquad \forall g\in F', f\in F'_g\cup V_g, \tag{8d}$$

$$\begin{aligned}E_g\le\;&E_f-x_{fg}(E^{X}(f)+E^{S}_{c}(f,g))\\&+(1-\beta)(\alpha E-(E_f-x_{fg}(E^{X}(f)+E^{S}_{c}(f,q))))\\&+\beta P^{c}\Delta t^{c}(f,g)+E\cdot(1-x_{fg})\end{aligned} \qquad \forall g\in F', f\in F'_g\cup V_g \tag{8e}$$

$$x_{fg}\in\{0,1\} \qquad \forall g\in F', f\in F'_g\cup V_g \tag{8f}$$

$$E^{X}(f)+E^{S}_{c1}(f)\le E_f\le E-E^{S}_{c1}(f) \qquad \forall f\in F' \tag{8g}$$

Eq. (8a) gives the objective function. Eqs. (8b) ensure that each vehicle is used at most once. Eqs. (8c) ensure that a flight is towed at most once, each flight from $F^{fix}$ is towed, and that vehicle flow is conserved. By excluding $f^{end}$, it is ensured that all ETVs end the day at the depot with a full battery **(A5)**. Eqs. (8d) connect the battery energy level between a flight or a towing vehicle and another flight. It considers both the case that there is no time to recharge the battery and that there is time to recharge it **(A4)**. Eqs. (8e) determine the battery energy level for subsequent flights if charging rate $\beta P^{c}$ is used **(A3)**. Finally, the domain of each decision variable is specified in Eqs. (8f) and (8g). From the $x$ variables in the solution, the list of to-be-towed flights $F_v$ is obtained.

### 5.1.4. Solution example for a simple problem instance

In order to illustrate the model formulation, we discuss a small example. We consider a single ETV $v$, operating at an airport with a gate node $g$, runway $r$, and charging station $c$. We discuss the schedule of $v$ between 6:00 and 9:00. We use $\Delta t^{reopt}=\Delta t^{fix}=30$ min and $\Delta t^{c}_{\min}=1$ h.

We consider two aircraft $F=\{a,d\}$ where $a$ is an arrival, and $d$ a departure. Both take 20 min to tow, and use 10% of the battery energy. The evolution of the ELDT of $a$ and the EOBT of $d$ is shown in Table 2: $a$ arrives earlier while $d$ is slightly delayed.

The evolution of the schedule of $v$ is given in Table 2 and Fig. 7. At 6:40, $v$ is charging, and has to charge until $t_v=7{:}20$. Either aircraft can be towed by $v$, such that $F'=\{a,d\}$ and $V'_a=V'_d=\{v\}$, but they cannot be towed both by $v$, such that $F'_a=F'_d=\emptyset$. Aircraft $a$ is assigned to $v$: $F_v=\{a\}$.

**Table 2**
Evolution of the schedule of ETV $v$ between 6:40 and 8:20. The ELDT and EOBT of aircraft $a$ and $d$ are shown, together with the optimization sets, as well as the state of $v$.

| t | Flight times | | Optimization sets | | | | | ETV state | | | | |
|---|---|---|---|---|---|---|---|---|---|---|---|---|
| | $ELDT_a$ | $EOBT_d$ | $F'$ | $F'_a$ | $F'_d$ | $V'_a$ | $V'_d$ | $n_v$ | $t_v$ | $E_v/E$ | $F_v$ | $S_v$ |
| 6:40 | 8:00 | 8:05 | a,d | ∅ | ∅ | v | v | c | 7:20 | 0.80 | a | Charging |
| 7:00 | 7:50 | 8:10 | a,d | ∅ | a | v | v | c | 7:20 | 0.80 | a,d | Charging |
| 7:20 | 7:45 | 8:10 | a,d | ∅ | a | v | v | c | 7:21 | 0.81 | a,d | Charging |
| 7:40 | 7:40 | 8:10 | d | ∅ | ∅ | ∅ | v | g | 8:00 | 0.69 | d | Towing |
| 8:00 | 7:40 | 8:10 | d | ∅ | ∅ | ∅ | v | g | 8:01 | 0.69 | d | Idle |
| 8:20 | 7:40 | 8:10 | ∅ | ∅ | ∅ | ∅ | ∅ | r | 8:30 | 0.59 | ∅ | Towing |

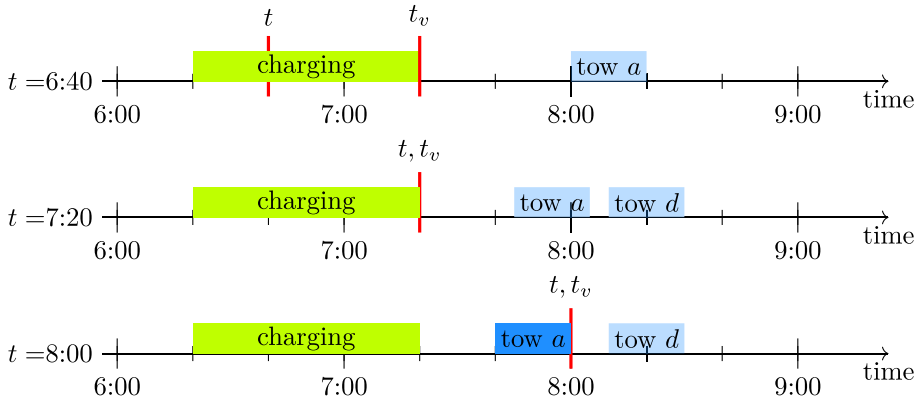


**Fig. 7.** Schedule of the ETV v at $t$ = 6:40, 7:20, and 8:00.

At 7:00 the ETV schedule is reoptimized. At this moment, $a$ is scheduled to arrive earlier, whereas $d$ is delayed, such that $F'_d = \{a\}$. Both $a$ and $d$ are assigned to $v$.

At 7:40, $v$ starts towing $a$. From this moment, $a$ is removed from $F'$, $F'_d$ and $F_v$. After this, $v$ tows aircraft $d$, which is also removed from $F'$ and $F_v$.

### 5.2. Dynamic ETV planning — execution and conflict resolution

While the ETV planning model from Section 5.1 assigns the ETVs to aircraft, it does not describe how to execute the schedule when the true values of $\tau^{\mathrm{P}}$ are revealed. This part of the framework is performed by Algorithm `ExecuteTows` (Alg. 2), which runs between global schedule reevaluations (Alg. 1). At each time $t$, the algorithm uses the latest available EOBTs and ELDTs to construct the most accurate pick-up time random variable $\tau^{\mathrm{P}}_f(t)$ to perform the schedule. As parameters, it requires a small time difference $\delta t$, and probability $\mathbb{P}_\theta$. It determines which flight to tow next and for how long to remain charging. In case the overlap time for two consecutively to-be-towed flights is positive, a scheduling conflict occurs, and the algorithm determines if a tow can be delayed or an aircraft is removed from the to-be-towed flights $F_v$.

Algorithm `ExecuteTows` is called every time an ETV $v$ is idle or charging, and provides it with a next action to perform. There are four possible actions which can be taken: tow an aircraft, drive to a location, remain idle, or keep charging. As input, it considers the current state of $v$, $(n_v, t_v, E_v, F_v, S_v)$. As before (Section 5.1.2), it takes the action $S'_v$ which yield the highest expected cost reduction, i.e. the one that minimize taxiing and delay cost. This action is provided to the ETV, together with the next state $(n'_v, t'_v, E'_v, F'_v, S'_v)$. A subroutine `NextFlight` 3 is used to determine the next to-be-towed flight.

## 6. Benchmark algorithms for ETV planning

In order to assess the quality of the proposed planning model, the *Stochastic pick-up time ETV planning*, we consider two benchmarks. These provide an upper and a lower bound on the objective function. They use the same framework as in Sections 5.1 and 5.2 but without using pick-up time random variables.

### 6.1. EOBT/ELDT Oracle ETV planning

The first benchmark assumes the AOBT and ALDT of all flights are known at the start of the day. With this information, there is no uncertainty in the problem and a planning can be made that uses the ETVs to maximum capacity. This provides an upper bound on the cost reduction the ETVs can provide.

**Algorithm 2:** `ExecuteTows` performs the ETV schedule

**Data:** ETV $v$ at state $t_v, n_v$, $E_v$, $F_v$, and $S_v$; time difference $\delta t$, probability $\mathbb{P}_\theta$.
**Result:** Action $S'_v$ and updated state $t'_v, n'_v, q'_v$ and $F'_v$

Let $\delta E$ be the amount by which the battery can be charged in $\delta t$ time;
Let $F'_v = F_v \setminus \{f : f \in F_v \cap F^{arr} \wedge \tau^{\mathrm{p}}_f < t_v\}$;
**if** $F_v \neq \emptyset$ **then**
  Get the next to-be-towed flight $f$ using Algorithm 3 ;
  Determine charging station $n^c = \arg\min_{n \in N^c}\{d^S(n_v, n) + d^S(n, n^{\mathrm{p}}_f)\}$;
  Determine the required charge to tow $f$ and reach a charging station $E_{min}$;
  Determine the available charging time $t_c$;
  **if** ($\mathbb{E}[t_c] > \Delta t^c_{min}$ *and* $n_v \neq n^c$) *or* $E_v < E_{min}$ **then**
    $S'_v$= "drive"; $n'_v = n^c$; $E'_v = E_v - \mathcal{E}(0, v_s) \cdot d^S(n_v, n^c)$; $t'_v = t_v + \frac{d^S(n_v, n^c)}{v_s}$; $F'_v = F_v$;
  **if** ($n_v = n^c$ *and* $E_v < E$ *and* $\mathbb{P}\left[t_v + \delta t + d^S(n_v, n^{\mathrm{p}}_f)/v_s < \tau^{\mathrm{p}}_f(t)\right] > \mathbb{P}_\theta$ ) *or* $E_v < E_{min}$ **then**
    $S'_v$= "Charge"; $n'_v = n_v$; $E'_v = E_v + \delta E$; $t'_v = t_v + \delta t$ ;
  **else**
    **if** $n_v = n^p_f$ **then**
      **if** $t_v$ *is smaller than the actual pick-up time of* $f$ **then**
        $S'_v$= "remain idle"; $n'_v = n_v$; $E'_v = E_v$; $t'_v = t_v + \delta t$ ;
      **else**
        $S'_v$= "tow $f$"; $n'_v = \tau^{\mathrm{d}}_f$; $E'_v = E_v - E^X(f)$; $t'_v = t_v + (\tau^{\mathrm{d}}_f(t) - \tau^{\mathrm{p}}_f(t))$; $F'_v \leftarrow F'_v \setminus \{f\}$ ;
      **end**
    **else**
      $S'_v$= "drive"; $n'_v = n^{\mathrm{p}}_f$; $E'_v = E_v - \mathcal{E}(0, v_s) \cdot d^S(n_v, n^{\mathrm{p}}_f)$; $t'_v = t_v + \frac{d^S(n_v, n^{\mathrm{p}}_f)}{v_s}$;
    **end**
  **end**
**else**
  Let $\tau^{\mathrm{p}}_f(t) = t_e$, $m_f = 0$, $n^{\mathrm{p}}_f = n^{\mathrm{d}}_f = n^{dep}$ and continue on line 10;
**end**

**Algorithm 3:** Algorithm `NextFlight` for finding the next to-be-towed flight in the ETV planning.

**Data:** Current state $(n_v, t_v, E_v, F_v, S_v)$ of the ETV.
**Result:** Next to-be-towed flight $h$

**if** $|F_v| = 1$ **then**
  $f$ is the only flight in $F_v$;
**else**
  Sort $F_v$ by $\mathbb{E}[\tau^{\mathrm{p}}_f(t_v)] - d^S(n_v, n^{\mathrm{p}}_f)/v^s$;
  Let $f$ be the first element of $F_v$;
  Set $h = f$;
  **if** $f \in F^{arr}$ **then**
    Sort the remaining flights of $F_v$ by $\mathbb{E}[\tau^{\mathrm{p}}_f(t_v)] - d^S(n^{\mathrm{d}}_f, n^{\mathrm{p}}_g)/v^s$;
    Let $g$ be the next flight with the lowest score ;
    **if** $g \in F^{arr}$ **then**
      **if** $c^{taxi}_f - c^{tow}_f + (c^{taxi}_g - c^{tow}_g) \times \mathbb{P}[\tau^o_{fg}(t_v) < 0] < c^{taxi}_g - c^{tow}_g$ **then**
        Set $h = g$ ;
    **else**
      **if** $\mathbb{E}[\tau^o_{fg}(t_v)]c^d_g > c^{taxi}_f - c^{tow}_f$ **then**
        set $h = g$;
    **end**
**end**

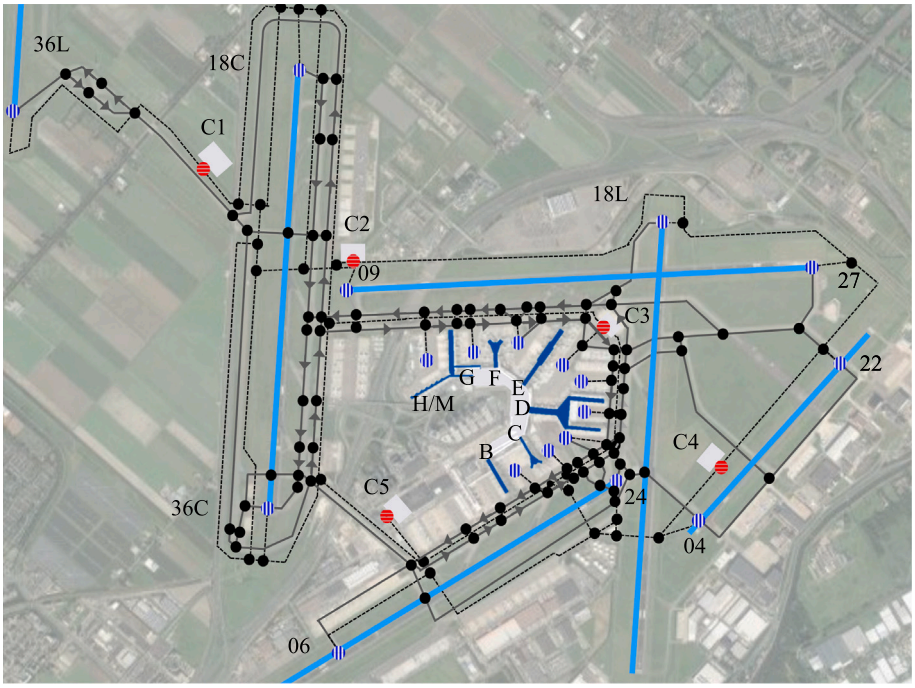


**Fig. 8.** Runways $N^R$ and gate nodes $N^G$, together with taxiways (solid lines), service roads (dashed lines) and charging stations $(C1, \ldots, C5)$ at AAS. The map is based on the Schiphol aerodrome charts (LVNL, 2024).

### 6.2. Point estimate pick-up time ETV planning

Using the mean values of stochastic parameters is an often used approach for optimization problems under uncertainty (Bertsimas and Sim, 2004). For dynamic ETV scheduling, this translates to using the latest available EOBT and ELDT values as average point estimates for the pick-up time. As such, the pick-up time is not an evolving random variable, but an evolving deterministic variable.

## 7. Case study: planning a fleet of ETVs at Amsterdam Airport Schiphol

*Airport taxi system and service roads*

Fig. 8 shows the layout of the airport, based on the Schiphol aerodrome charts (LVNL, 2024). The six runways and seven piers are represented by 19 nodes. These runway and gate nodes $N^{rg}$ are shown as vertically hatched circles. We assume that five charging stations are available at the airport, $N^{CS} = \{C1, C2, C3, C4, C5\}$, displayed as horizontally hatched circles. The ETV depot is located at charging station $n^{dep} = C5$. The taxiway and service road networks connect these nodes. They are displayed as solid and dashed lines, respectively. Some taxiways may be traversed in one direction only, this is indicated with arrowheads.

*ETV specifications*

We consider an ETV suitable to tow narrow-body aircraft (a.o. the B737, A320, and E190). Table 3 shows the assumed ETV specifications. Actual data on ETV energy usage is not available. As such, we consider the following energy consumption model for an ETV:

$$\mathcal{E}(v, m) = \mu^g(v) \cdot (m + m_v) \cdot g \qquad \text{with} \qquad \mu^g(v) = \mu^0 \cdot \left(1 + \tfrac{v}{v^0}\right) \tag{9}$$

where $\mathcal{E}$, the energy to tow over a unit distance, is a function of the velocity $v$, the mass of the ETV $m_v$ and towed aircraft $m$ (adapted from Daidzic (2017)). The rolling resistance coefficient $\mu^g$ is an increasing function of the velocity. Lastly, $g$ denotes the gravitational acceleration. This model assumes a constant towing velocity, see **(A2)**, on a horizontal terrain, and only considers rolling resistance. For this resistance, it assumes that the wheels of the ETV and aircraft are of a similar size. While the model does not account for acceleration/braking or the effect of the weather conditions, it provides a sufficient basis. Also, we note that the ETV planning framework can be considered regardless of the energy consumption model used.

**Table 3**
ETV and towing process parameters.

| Parameter | Explanation | Value | Parameter | Explanation | Value |
|---|---|---|---|---|---|
| $v^x$ [km/h] | Towing speed | 42.5 (Lukic et al., 2019) | $\Delta t^{\text{rel}}$ [s] | ETV disconnect time | 60 (Dieke-Meier and Fricke, 2012) |
| $P^c$ [kW] | Charging power | 100 (Baaren and Roling, 2019) | $\Delta t^{\text{pb}}$ [s] | Push-back time | 120 (Dieke-Meier and Fricke, 2012) |
| $m$ [$10^3$ kg] | ETV mass | 15 (Baaren and Roling, 2019) | $\alpha$ | Charging curve factor | 0.9 (Mitici et al., 2022) |
| $E$ [kWh] | Battery capacity | 400 (Baaren and Roling, 2019) | $\beta$ | Charging curve factor | 0.1 (Mitici et al., 2022) |
| $\Delta t^c_{\text{min}}$ [s] | Minimum charging time | 3600 | $\mu^0$ | Resistance factor | 0.1 (Daidzic, 2017) |
| $\Delta t^{\text{ec}}$ [s] | Engine cool-down time | 180 (Dzikus et al., 2013) | $v^0$ [km/h] | Resistance base velocity | 41 (Daidzic, 2017) |
| $\Delta t^{\text{con}}$ [s] | ETV connect-time | 60 | $v_s$ [km/h] | Service road velocity | 30 (Schiphol Health, Safety and Environment office, 2020) |

**Table 4**
Flights (arrivals and departures of narrow-body aircraft) at Schiphol airport, for 15 distinct day from 2023, where *Taxi cost* gives $\sum_{f\in F} c_f^{\text{taxi}} - c_f^{\text{tow}}$ for each day.

| Day | Flights | Taxi cost | Day | Flights | Taxi cost | Day | Flights | Taxi cost |
|---|---|---|---|---|---|---|---|---|
| Jul 13 | 1036 | € 606 828 | Sep 2 | 928 | € 535 086 | Oct 27 | 1051 | € 602 931 |
| Jul 28 | 1045 | € 604 120 | Sep 11 | 1050 | € 603 310 | Nov 2 | 811 | € 463 110 |
| Aug 3 | 1025 | € 588 295 | Sep 26 | 1029 | € 596 247 | Nov 11 | 967 | € 550 024 |
| Aug 12 | 954 | € 558 370 | Oct 3 | 1049 | € 602 082 | Nov 26 | 961 | € 547 371 |
| Aug 27 | 1021 | € 590 674 | Oct 12 | 1069 | € 614 734 | Dec 6 | 982 | € 571 295 |

*Taxiing and towing costs*

The taxiing and towing costs for a flight $f$ are determined as follows:

$$c_f^{\text{taxi}} = c^{kero} \cdot \frac{d^X(n_f^{\text{p}}, n_f^{\text{d}})}{v_x} \cdot FF_f \cdot m_f \tag{10}$$

$$c_f^{\text{tow}} = c^{elec} \cdot E^X(f), \tag{11}$$

where $c^{kero}$ is the cost of fuel consumption, $FF_f$ the fuel flow of the aircraft type of $f$ during taxiing, and $c^{elec}$ the cost of electricity. The cost $c^{kero}$ is the sum of the kerosene costs (€1.20 per litre International Air Transport Association, 2024), and the emission costs (€90 per tonne $CO_2$ Tiseo, 2024). The fuel flow $FF_f$ depends on the aircraft type and is taken from the ICAO *Engine Emissions Databank* (ICAO, 2023). The electricity cost $c^{elec}$ is set at €0.25 per kWh (Statistics Netherlands, 2023). The mass $m_f$ is the MTOW or EOW of the aircraft for departures and arrivals, respectively.

The delay costs for a flight $f$ depend on the aircraft type, and are assumed as per *European airline delay cost reference values* (Cook and Graham, 2015), updated to account for inflation (20% since 2015).

*Flight schedule*

We consider the flight schedules of 15 days during the summer and fall of 2023, spaced at regular intervals, see Table 4. All days of operation start at 6 AM and end at 6 AM on the next day. The flight data has been acquired using the Schiphol Developer Portal (Schiphol, 2023), from where the EOBTs and ELDTs are retrieved every minute.

*Obtaining the distributions of $\Delta OBT_\delta$ and $\Delta LDT_\delta$*

Using the flight data at Schiphol between July 1 and August 30 2023 (minus the days from Table 4), the distributions of the errors in the EOBT and ELDT have been determined. The random variables $\Delta\text{OBT}_\delta$ and $\Delta\text{LDT}_\delta$ are distributed accordingly. This is done as described in Section 3. Furthermore, in order to account for the different traffic levels during the day, $\Delta\text{OBT}_\delta$ and $\Delta\text{LDT}_\delta$ have been determined for every hour of the day separately. For each hour $h$, these are denoted by $\Delta\text{OBT}_\delta^h$ and $\Delta\text{LDT}_\delta^h$. To construct these, an arriving flight $f$ at time $t$ contributes $ALDT - ELDT_f(t)$ to the distribution of $\Delta\text{LDT}_\delta^h$, with $\delta = ELDT_f(t) - t$ and $h$. Conversely, to determine $\tau_f^{\text{p}}(t)$ (Eq. (1)), the random variable $\Delta\text{LDT}_\delta^h$ is used where $h$ is the hour of $ELDT_f(t)$.

*Experimental setup*

The model from Section 5.1 has been implemented in the Gurobi Optimizer 10.0.2, on a pc with 17 AMD Ryzen 7-1700X processors. In order to accelerate the optimization, the algorithm is hot-started with a greedy assignment. To obtain the final assignment, the model is optimized for a maximum of 5 min. Furthermore, a time interval of $\Delta t^{fix} = 45$ min is used (Assumption **(A12)**). Lastly, the probabilities $\mathbb{P}_\phi = 0.05$ (to define $F'$), $\mathbb{P}_\theta = 0.95$ (in Eq. (5) and Algorithm 2), and $\delta = 1$ minute are used.

**Table 5**
Performance of the Stochastic pick-up time ETV planning algorithm (Section 5), using a 5 ETV fleet on July 13, 2023. Values of $\Delta t^{reopt}$ between 15 and 45 min are tested. Let $F^{tow}$ be the set of towed aircraft. *Emission reduction* gives $\sum_{f \in F^{tow}} c_f^{\text{taxi}} - c_f^{\text{tow}}$ (in €), *delay* the delay caused by towing operations ($\sum_f c_f^{\text{d}}$); *cost reduction* gives $\sum_{f \in F^{tow}} c_f^{\text{taxi}} - c_f^{\text{tow}} - c_f^{\text{d}}$.

| $\Delta t^{reopt}$ [min] | 15 | 20 | 25 | 30 | 35 | 40 | 45 |
|---|---|---|---|---|---|---|---|
| Emission reduction [€] | 79 087 | 80 151 | 80 871 | 76 771 | 76 564 | 78 335 | 75 622 |
| Delay [€] | 10 343 | 11 465 | 10 521 | 6 441 | 7 894 | 5 540 | 5 437 |
| Cost reduction [€] | 68 744 | 66 554 | 70 350 | 70 330 | 68 652 | 75 795 | 70 185 |

**Table 6**
Performance of the three ETV planning algorithms (Section 5), using a 5 ETV fleet on July 13, 2023. Let $F^{tow}$ be the set of towed aircraft. *Emission reduction* gives $\sum_{f \in F^{tow}} c_f^{\text{taxi}} - c_f^{\text{tow}}$ (in € and as percentage of total costs), *delay* the delay caused by towing operations (both in minutes and as $\sum_f c_f^{\text{d}}$); *cost reduction* gives $\sum_{f \in F^{tow}} c_f^{\text{taxi}} - c_f^{\text{tow}} - c_f^{\text{d}}$.

| ETV planning method | Emission reduction | | Delay | | Cost reduction | |
|---|---|---|---|---|---|---|
| | [€] | [%] | [€] | [min] | [€] | [%] |
| EOBT/ELDT Oracle (Section 6.1) | 107 387 | 18.2 | 708 | 38 | **106 678** | 17.6 |
| Stochastic pick-up time (Section 5) | 78 335 | 12.9 | 5 540 | 60 | **72 795** | 12.0 |
| Point estimate pick-up time (Section 6.2) | 88 215 | 14.6 | 29 315 | 319 | **58 899** | 9.7 |

**Table 7**
Number of flights towed, using the three ETV planning algorithms presented in Section 5, using a 5 ETV fleet on July 13, 2023, with $c^{\text{taxi}} - c^{\text{d}}$ the total emission cost reduction.

| ETV planning method | All flights | | Arrivals | | | |
|---|---|---|---|---|---|---|
| | # Tows | $c^{\text{taxi}} - c^{\text{tow}}$ | # Tows | | $c^{\text{taxi}} - c^{\text{tow}}$ | |
| | [–] | [€] | [–] | [%] | [€] | [%] |
| EOBT/ELDT Oracle (Section 6.1) | 199 | 110 387 | 82 | 41.2 | 54 949 | 49.8 |
| Stochastic pick-up time (Section 5) | 147 | 78 335 | 72 | 49.0 | 42 692 | 54.5 |
| Point estimate pick-up time (Section 6.2) | 172 | 88 215 | 52 | 28.6 | 32 683 | 37.3 |

## 8. Case study: Numerical results

### 8.1. Sensitivity analysis of $\Delta t^{reopt}$

In order to find proper values for the schedule reevaluation time $\Delta t^{reopt}$ (Algorithm 1), a sensitivity analysis has been performed. This is done using the flight data of July 13, 2023, and with a fleet of 5 ETVs (the same experiment as in Section 8.2).

Table 5 shows the results of the parameter tuning. For each value of $\Delta t^{reopt}$, the emission cost reduction $c^{\text{taxi}} - c^{\text{tow}}$, the delay cost incurred $c^{\text{d}}$, and total cost reduction $c^{\text{taxi}} - c^{\text{tow}} - c^{\text{d}}$ are given. Using lower values of $\Delta t^{reopt}$ results in towing more aircraft, but also increases the delays caused by ETVs. Overall, the value of $\Delta t^{reopt} = 40$ min maximizes the total cost reduction, and is used in the remainder of this section.

### 8.2. Dispatching ETVs on the 13th of July 2023 at Schiphol

We illustrate our proposed ETV planning approach considering the flight schedule of July 13, 2023. We consider a fleet of 5 ETVs. On this day, 1036 narrow-body aircraft arrived and departed from Schiphol, with a total taxiing emission cost of €606 828.

The results are given in Table 6. Using the *Stochastic pick-up time ETV planning*, 147 flights are towed, of which 72 arrivals and 75 departures, and a total cost reduction of **€72 795** is achieved. The total $c^{\text{taxi}} - c^{\text{tow}}$ of the towed flights is €78 335, which is 12.9% of the total during this day. Because of towing, flights were delayed by a total of 60 min (on average 1 min/departure), resulting in a cost of €5540.

The *EOBT/ELDT Oracle ETV planning* (Section 6.1) achieves a cost reduction of **€106 678** by towing 199 flights. The *Point estimate pick-up time ETV planning* (Section 6.2) achieves a cost reduction of **€58 899**. Using this method, more flights are towed (182 against 134), but a similar total emission cost reduction $c^{\text{taxi}} - c^{\text{tow}}$ is achieved (€88 215 against €78 335). The major flaw of the *Point estimate* ETV planning method is the high delay costs it incurs, almost €30 000 (or 319 min). Finally, Table 7 shows that a relative large share of the tows performed in this case were arriving flights (49% against 41% with perfect- and 29% with point estimate information). This is due to the smaller uncertainty in pick-up time of the arrival flights, see also Fig. 1.

The ETV schedules are shown in Fig. 9 for the *EOBT/ELDT Oracle* (9(a)), *Point estimate pick-up time* (9(b), 9(c)), and *Stochastic pick-up time* (9(d), 9(e)) ETV planning. Towing an aircraft without delays is shown as solid blue bars, delayed towing as dotted red bars, charging as hatched green bars, and driving as light-grey bars. The current time $t$ and the next optimization time $t + \Delta t^{reopt}$ are shown as vertical dashed lines. The schedule given by the *EOBT/ELDT Oracle ETV planning* does not change during the day, the schedules given by the *Stochastic pick-up time* and *Point estimate pick-up time ETV planning* algorithms are shown at two different times. The *Point estimate pick-up time ETV planning* leads to large delays, see Fig. 9(c) and ETV 2 after 14:30. It also shows consecutively

**Table 8**
Average performance *per ETV per day* of the three ETV planning methods, considering the flight schedules of the days in Table 4. ETV fleets of 5, 20, and 40 vehicles are shown. The *Cost reduction* is the total $c^{\text{taxi}} - c^{\text{tow}} - c^{\text{d}}$ of all towed flights.

| ETV planning method | Cost reduction | Delay | Tows | Arrivals | | Departures | |
|---|---|---|---|---|---|---|---|
| | [€] | [min] | [#] | [#] | [%] | [#] | [%] |
| *5 ETVs* | | | | | | | |
| EOBT/ELDT Oracle (Section 6.1) | 24 717 | 8.3 | 44.9 | 18.0 | 40.1 | 26.9 | 59.9 |
| Stochastic pick-up time (Section 5) | 17 364 | 12.4 | 27.8 | 13.6 | 48.9 | 14.2 | 51.1 |
| Point estimate pick-up time (Section 6.2) | 15 655 | 47.2 | 35.8 | 13.0 | 36.2 | 22.8 | 63.8 |
| *20 ETVs* | | | | | | | |
| EOBT/ELDT Oracle (Section 6.1) | 19 955 | 3.1 | 34.3 | 16.4 | 47.8 | 17.9 | 52.2 |
| Stochastic pick-up time (Section 5) | 14 760 | 8.8 | 25.1 | 12.4 | 49.2 | 12.8 | 50.8 |
| Point estimate pick-up time (Section 6.2) | 13 144 | 24.0 | 26.6 | 12.0 | 45.0 | 14.6 | 55.0 |
| *40 ETVs* | | | | | | | |
| EOBT/ELDT Oracle (Section 6.1) | 13 788 | 1.6 | 23.9 | 11.2 | 46.7 | 12.7 | 53.3 |
| Stochastic pick-up time (Section 5) | 11 443 | 3.7 | 20.3 | 9.8 | 48.4 | 10.5 | 51.6 |
| Point estimate pick-up time (Section 6.2) | 9 771 | 7.4 | 18.4 | 8.9 | 48.4 | 9.5 | 51.6 |

delayed tows: one flight is delayed, causing the next tow to be delayed as well. These are largely absent when stochastic pick-up times were accounted for (Fig. 9(d)).

### 8.3. Dispatching ETVs at Schiphol considering 15 distinct days

To assess the general performance of the *Stochastic pick-up time ETV planning*, all three planning methods have been applied on 15 days of operations (see Table 4). For each day and each planning method, we consider ETV fleets from 0 up to 50 vehicles.

For each day of operations, fleet size, and planning method, we determined the taxi cost reductions $c^{\text{taxi}} - c^{\text{tow}}$ and the delay costs $c^{\text{d}}$ of all towed flights. Fig. 10 shows the median and 10–90 percentiles of these results for all methods per fleet size. It shows the emission cost reduction $c^{\text{taxi}} - c^{\text{tow}}$ (10(a)), delay cost $c^{\text{d}}$ (10(b)), and total cost reduction $c^{\text{taxi}} - c^{\text{tow}} - c^{\text{d}}$ (10(c)). Additionally, in Figs. 10(a) and 10(c), the average maximum emission cost reduction of all flights are shown as a horizontal line.

Fig. 10 shows a considerable difference in the performance of the planning algorithms for different ETV fleet sizes. The difference between the *Stochastic/Point-estimate pick-up time* and the *EOBT/ELDT Oracle ETV planning* methods is largest during the scale-up of the ETV fleet: between 15 and 40 ETVs. At this stage there are not enough vehicles to tow a large fraction of the aircraft. In this case, the *Point estimate pick-up time* plan is able to tow more aircraft (10(a)), but incurs an especially large delay cost (10(b)). Both show an increasing delay cost up to 30 ETVs, after which it decreases to €10.000 for the *Stochastic pick-up time* and €20.000 for the *Point-estimate pick-up time ETV planning* (10(b)). Above 40 ETVs, the difference in cost reduction stagnates around €90.000 for the *Stochastic pick-up time ETV planning* method and €150.000 for the *Point estimate pick-up time ETV planning* method (10(c)). This is due to the loss of performance due to imperfect information.

Table 8 in detail the obtained results for fleets of 5, 20, and 40 ETVs. It shows the average results per ETV (i.e., cost reduction, delay, number of towing tasks per ETV), over all 15 days.

The *Stochastic pick-up time ETV planning* method leads to higher cost reductions than the *Point estimate pick-up time ETV planning*: €1600 per ETV per day, irrespective of the fleet size. Moreover, the gap between these two approaches and the *EOBT/ELDT Oracle ETV planning* decreases from over 29% to 15% for large fleet sizes. This is largely due to the reduction in delay costs. Also, the number of towed aircraft for the *Stochastic pick-up time ETV planning* decreases less then in the two other methods: from 38.1 to 15.1. This is due to the larger buffers used by this approach, see also Fig. 9. This approach also has a preference for towing arrivals for a small fleet of ETVs is considered (as seen in Section 8.2). This is no longer the case when we consider large fleets of ETVs.

Finally, when considering fleet sizes of 0–50 ETVs, the *Stochastic pick-up time ETV planning* method is able to achieve a cost reduction of **€12 104** on average per ETV per day. This is 79.5% of the cost reduction achieved by the *EOBT/ELDT Oracle ETV planning* method, that achieved a reduction of **€15 225**. This is a clear improvement over the *Point estimate pick-up time ETV planning* method, which achieves a cost reduction of **€10 276** (67.5% of the *EOBT/ELDT Oracle*).

## 9. Conclusions

Our paper proposes a stochastic and dynamic framework to dispatch a fleet of electric towing vehicles (ETVs) to tow aircraft by accounting for uncertain arrival and departure times of aircraft: the *Stochastic pick-up time ETV planning*. A planning is made indicating which aircraft is towed by which ETV and when the ETVs recharge their batteries. We create a schedule that maximizes fuel savings by replacing conventional taxiing with ETV towing. At the same time, we minimize the delay induced by the use of ETVs. This is done using a rolling horizon approach, where the stochastic arrival and departure times are updated periodically. From a methodological perspective, our approach extends the E-VRP-TW problem to instances with stochastic and dynamically evolving start times of time windows.

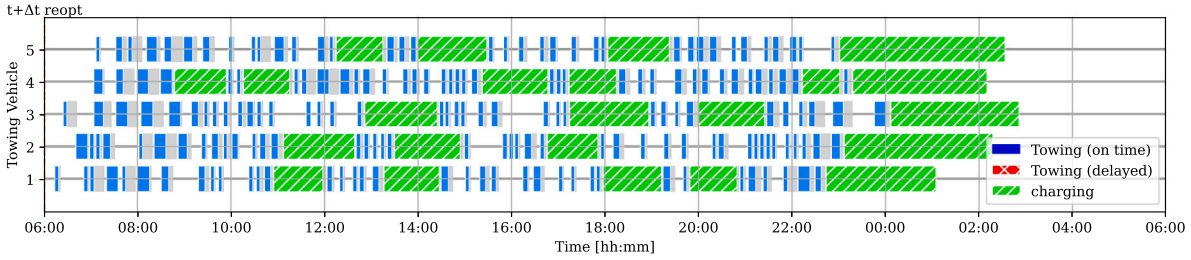


(a) *EOBT/ELDT Oracle ETV planning*

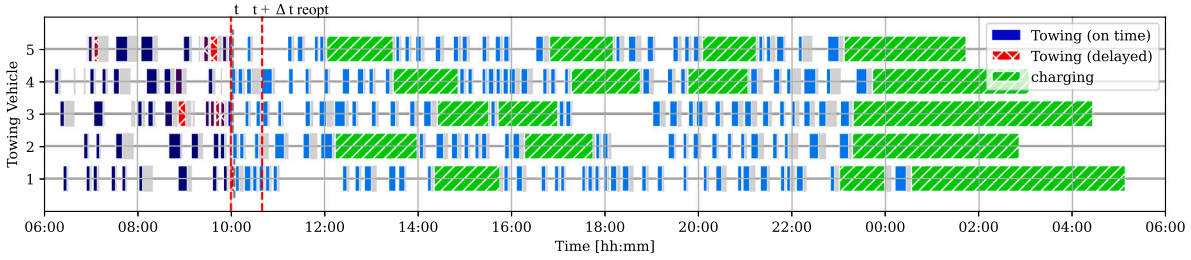


(b) *Point estimate pick-up time ETV planning*, situation at $t$ = 10:00 AM, July 13

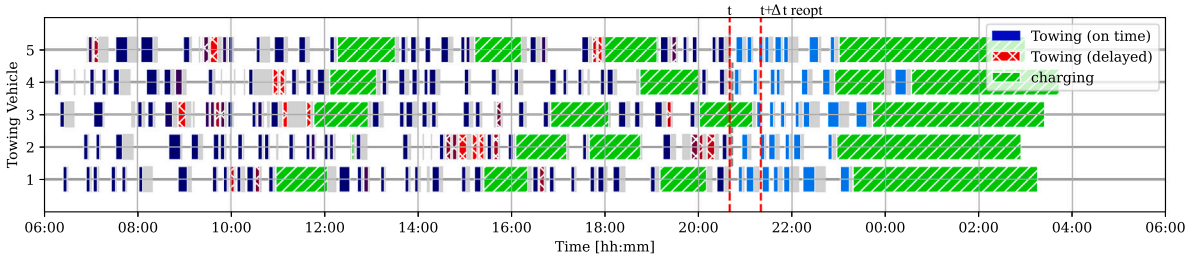


(c) *Point estimate pick-up time ETV planning*, situation at $t$ = 8:40 PM, July 13

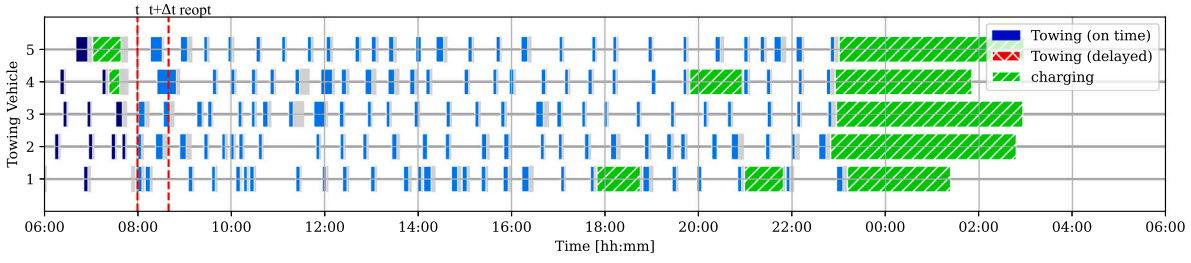


(d) *Stochastic pick-up time ETV planning*, situation at $t$ = 8 AM, July 13

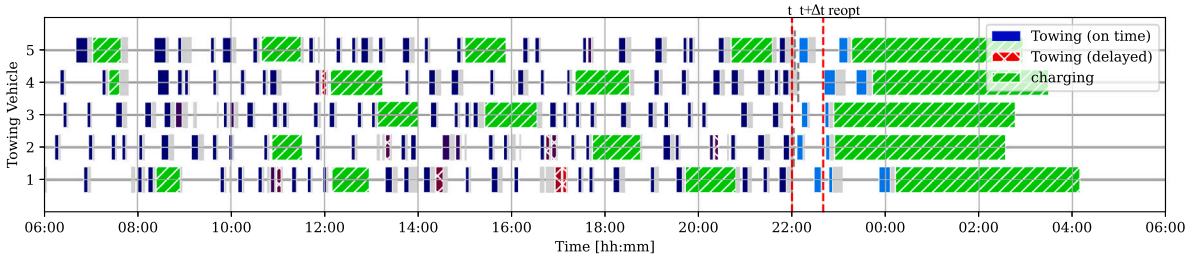


(e) *Stochastic pick-up time ETV planning*, situation at $t$ = 10 PM, July 13

**Fig. 9.** ETV planning for July 13, 2023 for a fleet of 5 ETVs, using the three ETV planning algorithms from Section 5.

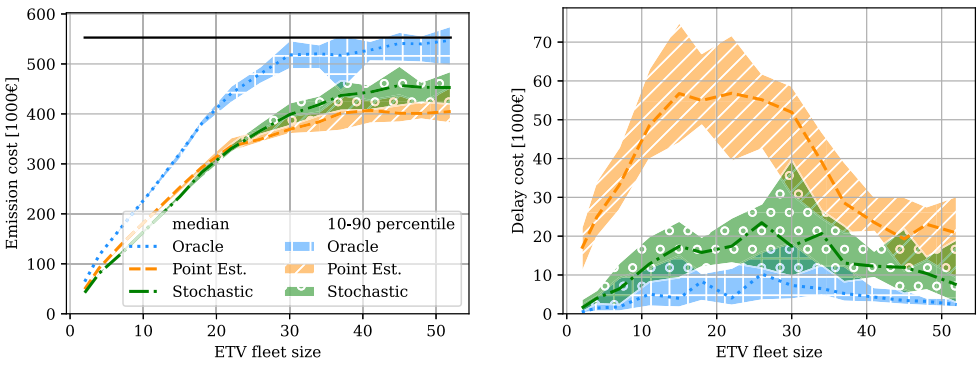


(a) Emission cost reduction

(b) Delay cost incurred

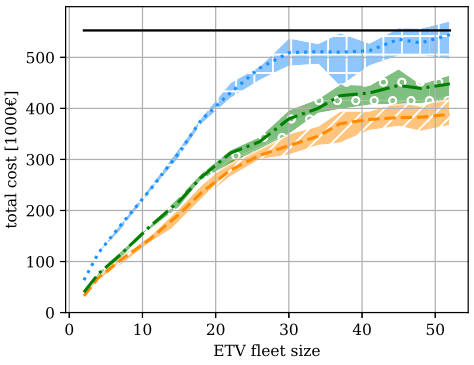


(c) Total cost reduction

**Fig. 10.** Cost reduction achieved by dispatching ETV fleets between 0 and 50 vehicles at *Schiphol* airport, for 15 days of operations (Table 4). The medians are shown as a line, the 10–90 percentiles as a shaded area.

The *Stochastic pick-up time ETV planning* framework is illustrated for several days of operations from 2023 at Amsterdam Airport *Schiphol*. We consider a fleet of ETVs that tow narrow-body aircraft. We obtain schedules for ETV towing tasks and battery charging, which are updated periodically. Our approach is benchmarked against: (i) an approach that assumes a priori full knowledge of the actual arrival/departure times (*EOBT/ELDT Oracle ETV planning*), and (ii) an approach which assumes average point estimates of the arrival/departure times (*Point Estimate pick-up time ETV planning*). The results show that our proposed approach achieves an average taxiing cost reduction of €12 104 per ETV per day (79.5% of the *EOBT/ELDT Oracle*), compared with €10 276 cost reduction for the *Point Estimate pick-up time* planning (67.5% of the *EOBT/ELDT Oracle*, 84.9% of our proposed approach).

As future work, we aim to consider additional sources of disruption, such as decreased battery performance or changing runway configurations. Furthermore, the possibility of simultaneously minimizing taxiing/towing costs and ETV driving costs can be studied. To further improve the performance of the algorithm, hyperparameter tuning can be performed. Lastly, we plan to investigate effective policies for runway usage that boost environmental benefits.

## CRediT authorship contribution statement

**Simon van Oosterom:** Writing – original draft, Visualization, Methodology, Investigation, Conceptualization. **Mihaela Mitici:** Writing – original draft, Supervision, Methodology, Conceptualization.

## Appendix. Nomenclature

An overview of the used nomenclature can be found in Table A.9.

**Table A.9**
Overview of used nomenclature.

| | |
|---|---|
| **Sets** | |
| $T$ | Day of operations |
| $V$ | ETV fleet |
| $N$ | Nodes in the airport road network |
| $N^{rg}$ | Runway/gate nodes in $N$ |
| $N^{c}$ | Charging station nodes in $N$ |
| $A$ | Arcs in the airport road network |
| $A^{X}$ | Taxiway roads in $A$ |
| $A^{S}$ | Service roads in $A$ |
| $F$ | Arriving and departing flights |
| $F^{arr}$ | Arriving flights |
| $F^{dep}$ | Departing flights |
| $F'$ | Flights which can still be towed after the current time |
| $F'_f$ | Flights which can be towed by the same ETV before towing $f$ |
| $V_f$ | ETVs which can tow flight $f$ given their current state |
| $F'^{c}_f$ | Flights which can be towed before $f$ by the same ETV, with time to recharge between the tows |
| **ETV parameters** | |
| $E$ | ETV battery energy capacity |
| $\mathcal{E}$ | ETV energy usage per unit distance |
| $P^{c}$ | Recharge power |
| $\alpha, \beta$ | Bilinear charging cure coefficients |
| $v^{x}$ | Towing velocity |
| $v^{s}$ | Driving velocity |
| $\Delta t^{\text{ec}}$ | Engine cool-down time |
| $\Delta t^{\text{con}}$ | ETV connect time |
| $\Delta t^{\text{rel}}$ | ETV release time |
| $\Delta t^{\text{pb}}$ | Aircraft push-back time |
| $\mu^{s}(v)$ | Rolling resistance coefficient at velocity $v$ |
| $\mu^{0}, v^{0}$ | Rolling resistance coefficients |
| **Airport parameters** | |
| $n^{dep}$ | ETV depot node |
| $d^{X}$ | Taxiway distance |
| $d^{S}$ | Service road distance |
| **Aircraft parameters** | |
| $n^{\text{p}}_f$ | Pick-up location of aircraft $f$ |
| $n^{\text{d}}_f$ | Drop-off location of $f$ |
| $m_f$ | Mass of $f$ |
| $FF_f$ | Fuel flow of $f$ while towing |
| $ALDT_f$ | Actual landing time of $f$ |
| $ELDT_f(t)$ | Estimated landing time of $f$ at time $t$ |
| $\Delta\text{LDT}_\delta$ | Random variable of $ALDT - ELDT$ at $\delta$ time before the $ELDT$ |
| $AOBT_f$ | Actual off-block time of $f$ |
| **Aircraft parameters** (ctd.) | |
| $EOBT_f(t)$ | Estimated off-block time of $f$ at $t$ |
| $\Delta\text{OBT}_\delta$ | Random variable of $AOBT - EOBT$ at $\delta$ time before the $EOBT$ |
| $\tau^{\text{p}}_f(t)$ | Desired pick-up time random variable of $f$ at time $t$ |
| $\tau^{\text{d}}_f(t)$ | Desired drop-off time random variable of $f$ at time $t$ |
| $\tau^{\text{o}}_{fg}(t)$ | Overlap time random variable at time $t$ if $f$ and $g$ are consecutively towed by the same ETV |
| **ETV planning parameters** | |
| $\Delta t^{c}(f,g)$ | Recharge time between towing aircraft $f$ and $g$ |
| $\Delta t^{fix}$ | Schedule fix time for departing aircraft |
| $\Delta t^{reopt}$ | Time between ETV planning reevaluations |
| $\Delta t^{c}_{\text{min}}$ | Minimum allowed recharge time |
| $n^{\text{a}}_v$ | First available location of ETV $v$ |
| $E_v$ | Battery energy of $v$ at first available moment |
| $\tau^{\text{a}}_v(t)$ | First available moment of ETV $v$ at current time $t$ |
| $f_{end}$ | Artificial flight |
| $F^{fix}$ | Departing flights which have to be assigned to an ETV |
| $E^{X}(f)$ | Energy required to tow $f$ |
| $E^{S}(f,g)$ | Energy required to drive from the drop-off of $f$ to the pick-up of $g$ |
| $E^{S}_{c}(f,g)$ | Energy required to drive from the drop-off of $f$ to the pick-up of $g$ via a charging station |
| $E^{S}_{c1}(f)$ | Energy required to drive from the drop-off point of $f$ to the furthest charging station |
| $\delta t$ | ETV planning reevaluation time |

(*continued on next page*)

**Table A.9** (*continued*).

| | |
|---|---|
| **Cost parameters** | |
| $c_f^{\text{taxi}}$ | Cost of letting aircraft $f$ taxi |
| $c_f^{\text{tow}}$ | Cost of towing $f$ |
| $c_f^{\text{d}}$ | Cost of delaying $f$ for a unit time |
| $c_{fg}(t)$ | Cost reduction of towing $f$ directly before $g$, given an overlap time $t$ |
| $c^{kero}$ | Kerosene cost |
| $c^{elec}$ | Electricity cost |
| **Model variables** | |
| $x_{fg}$ | Binary, true if aircraft $f$ is towed directly before $g$ by the same ETV |
| $E_f$ | ETV battery charge directly after towing $f$ |

## References


Baaren, E.v., Roling, P.C., 2019. Design of a zero emission aircraft towing system. In: AIAA Aviation 2019 Forum. In: AIAA AVIATION Forum, American Institute of Aeronautics and Astronautics, http://dx.doi.org/10.2514/6.2019-2932, URL https://arc.aiaa.org/doi/10.2514/6.2019-2932.

Bertsimas, D., Sim, M., 2004. The price of robustness. Oper. Res. http://dx.doi.org/10.1287/opre.1030.0065, URL https://pubsonline.informs.org/doi/abs/10.1287/opre.1030.0065. Publisher: INFORMS.

Bräysy, O., Gendreau, M., 2005a. Vehicle routing problem with time windows, part I: Route construction and local search algorithms. Transp. Sci. 39 (1), 104–118. http://dx.doi.org/10.1287/trsc.1030.0056, URL http://pubsonline.informs.org/doi/abs/10.1287/trsc.1030.0056.

Bräysy, O., Gendreau, M., 2005b. Vehicle routing problem with time windows, part II: Metaheuristics. Transp. Sci. 39 (1), 119–139. http://dx.doi.org/10.1287/trsc.1030.0057, URL http://pubsonline.informs.org/doi/abs/10.1287/trsc.1030.0057.

Charnes, A., Cooper, W.W., 1959. Chance-constrained programming. Manage. Sci. 6 (1), 73–79. http://dx.doi.org/10.1287/mnsc.6.1.73, URL https://pubsonline.informs.org/doi/abs/10.1287/mnsc.6.1.73. Publisher: INFORMS.

Chen, S., Wu, L., Ng, K.K.H., Liu, W., Wang, K., 2024. How airports enhance the environmental sustainability of operations: A critical review from the perspective of Operations Research. Transp. Res. E 183, 103440. http://dx.doi.org/10.1016/j.tre.2024.103440, URL https://www.sciencedirect.com/science/article/pii/S1366554524000309.

Conrad, R., Figliozzi, M.A., 2011. The Recharging Vehicle Routing Problem. Institute of Industrial & System Engineers, URL https://web.cecs.pdx.edu/~maf/Conference_Proceedings/2011_The_Recharging_Vehicle_Routing_Problem.pdf.

Cook, A., Graham, T., 2015. European Airline Delay Cost Reference Values. Tech. Rep., Eurocontrol, URL https://www.eurocontrol.int/publication/european-airline-delay-cost-reference-values.

Daidzic, N.E., 2017. Determination of taxiing resistances for transport category airplane tractive propulsion. Adv. Aircr. Spacecr. Sci. 4 (6), 651–677. http://dx.doi.org/10.12989/aas.2017.4.6.651, URL http://koreascience.or.kr/article/JAKO201732060819214.page. Publisher: Techno-Press.

Desaulniers, G., Errico, F., Irnich, S., Schneider, M., 2016. Exact algorithms for electric vehicle-routing problems with time windows. Oper. Res. 64 (6), 1388–1405. http://dx.doi.org/10.1287/opre.2016.1535, URL https://pubsonline.informs.org/doi/10.1287/opre.2016.1535. Publisher: INFORMS.

Diefenbach, H., Emde, S., Glock, C.H., 2023. Multi-depot electric vehicle scheduling in in-plant production logistics considering non-linear charging models. European J. Oper. Res. 306 (2), 828–848. http://dx.doi.org/10.1016/j.ejor.2022.06.050, URL https://www.sciencedirect.com/science/article/pii/S0377221722005252.

Dieke-Meier, F., Fricke, H., 2012. Expectations from a steering control transfer to cockpit crews for aircraft pushback. In: Proceedings of the 2nd International Conference on Application and Theory of Automation in Command and Control Systems. ATACCS '12, IRIT Press, Toulouse, FRA, pp. 62–70.

Dzikus, N.M., Wollenheit, R., Schaefer, M., Gollnick, V., 2013. The benefit of innovative taxi concepts: The impact of airport size, fleet mix and traffic growth. In: 2013 Aviation Technology, Integration, and Operations Conference. In: AIAA AVIATION Forum, American Institute of Aeronautics and Astronautics, http://dx.doi.org/10.2514/6.2013-4212, URL https://arc.aiaa.org/doi/10.2514/6.2013-4212.

Erdoğan, S., Miller-Hooks, E., 2012. A green vehicle routing problem. Transp. Res. E 48 (1), 100–114. http://dx.doi.org/10.1016/j.tre.2011.08.001, URL https://www.sciencedirect.com/science/article/pii/S1366554511001062.

EUROCONTROL, 2023a. Network Manager Annual Report 2022. Tech. Rep., EUROCONTROL, Brussels, URL https://www.eurocontrol.int/publication/network-manager-annual-report-2022.

EUROCONTROL, 2023b. Annual Network Operations Report 2022. Tech. Rep., EUROCONTROL, Brussels, URL https://www.eurocontrol.int/publication/annual-network-operations-report-2022.

Figliozzi, M.A., 2010. An iterative route construction and improvement algorithm for the vehicle routing problem with soft time windows. Transp. Res. C 18 (5), 668–679. http://dx.doi.org/10.1016/j.trc.2009.08.005, URL https://www.sciencedirect.com/science/article/pii/S0968090X09001119.

Hiermann, G., Puchinger, J., Ropke, S., Hartl, R.F., 2016. The electric fleet size and mix vehicle routing problem with time windows and recharging stations. European J. Oper. Res. 252 (3), 995–1018. http://dx.doi.org/10.1016/j.ejor.2016.01.038, URL https://www.sciencedirect.com/science/article/pii/S0377221716000837.

ICAO, 2023. ICAO Aircraft Engine Emissions Databank. Tech. Rep., URL https://www.easa.europa.eu/en/domains/environment/icao-aircraft-engine-emissions-databank.

International Air Transport Association, 2022. Global Outlook for Air Transport. Tech. Rep., IATA, Montreal, URL https://www.iata.org/en/iata-repository/publications/economic-reports/global-outlook-for-air-transport---december-2022/.

International Air Transport Association, 2024. Jet fuel price monitor. URL https://www.iata.org/en/publications/economics/fuel-monitor/.

Keskin, M., Çatay, B., 2016. Partial recharge strategies for the electric vehicle routing problem with time windows. Transp. Res. C 65, 111–127. http://dx.doi.org/10.1016/j.trc.2016.01.013, URL https://www.sciencedirect.com/science/article/pii/S0968090X16000322.

Keskin, M., Çatay, B., 2018. A matheuristic method for the electric vehicle routing problem with time windows and fast chargers. Comput. Oper. Res. 100, 172–188. http://dx.doi.org/10.1016/j.cor.2018.06.019, URL https://www.sciencedirect.com/science/article/pii/S0305054818301849.

Khadilkar, H., Balakrishnan, H., 2012. Estimation of aircraft taxi fuel burn using flight data recorder archives. Transp. Res. D 17 (7), 532–537. http://dx.doi.org/10.1016/j.trd.2012.06.005, URL https://www.sciencedirect.com/science/article/pii/S1361920912000612.

Lam, E., Desaulniers, G., Stuckey, P.J., 2022. Branch-and-cut-and-price for the electric vehicle routing problem with time windows, piecewise-linear recharging and capacitated recharging stations. Comput. Oper. Res. 145, 105870. http://dx.doi.org/10.1016/j.cor.2022.105870, URL https://www.sciencedirect.com/science/article/pii/S0305054822001423.

Lee, D.S., Fahey, D.W., Skowron, A., Allen, M.R., Burkhardt, U., Chen, Q., Doherty, S.J., Freeman, S., Forster, P.M., Fuglestvedt, J., Gettelman, A., De León, R.R., Lim, L.L., Lund, M.T., Millar, R.J., Owen, B., Penner, J.E., Pitari, G., Prather, M.J., Sausen, R., Wilcox, L.J., 2021. The contribution of global aviation to anthropogenic climate forcing for 2000 to 2018. Atmos. Environ. 244, 117834. http://dx.doi.org/10.1016/j.atmosenv.2020.117834, URL https://www.sciencedirect.com/science/article/pii/S1352231020305689.

Lorini, S., Potvin, J.-Y., Zufferey, N., 2011. Online vehicle routing and scheduling with dynamic travel times. Comput. Oper. Res. 38 (7), 1086–1090. http://dx.doi.org/10.1016/j.cor.2010.10.019, URL https://www.sciencedirect.com/science/article/pii/S0305054810002480.

Lukic, M., Giangrande, P., Hebala, A., Nuzzo, S., Galea, M., 2019. Review, challenges, and future developments of electric taxiing systems. IEEE Trans. Transp. Electrif. 5 (4), 1441–1457. http://dx.doi.org/10.1109/TTE.2019.2956862, Conference Name: IEEE Transactions on Transportation Electrification.

LVNL, 2024. EHAM airport profile. URL https://eaip.lvnl.nl/web/2023-04-06-AIRAC/html/eAIP/EH-AD-2.EHAM-en-GB.html.

Messaoud, E., 2023. A chance constrained programming model and an improved large neighborhood search algorithm for the electric vehicle routing problem with stochastic travel times. Evol. Intell. 16 (1), 153–168. http://dx.doi.org/10.1007/s12065-021-00648-0.

Mitici, M., Pereira, M., Oliviero, F., 2022. Electric flight scheduling with battery-charging and battery-swapping opportunities. EURO J. Transp. Logist. 11, 100074. http://dx.doi.org/10.1016/j.ejtl.2022.100074.

Nikoleris, T., Gupta, G., Kistler, M., 2011. Detailed estimation of fuel consumption and emissions during aircraft taxi operations at Dallas/Fort worth international airport. Transp. Res. D 16 (4), 302–308. http://dx.doi.org/10.1016/j.trd.2011.01.007, URL https://www.sciencedirect.com/science/article/pii/S1361920911000198.

Omidvar, A., Tavakkoli-Moghaddam, R., 2012. Sustainable vehicle routing: Strategies for congestion management and refueling scheduling. In: 2012 IEEE International Energy Conference and Exhibition. ENERGYCON, IEEE, Florence, Italy, pp. 1089–1094. http://dx.doi.org/10.1109/EnergyCon.2012.6347732, URL http://ieeexplore.ieee.org/document/6347732/.

van Oosterom, S., Mitici, M., Hoekstra, J., 2023. Dispatching a fleet of electric towing vehicles for aircraft taxiing with conflict avoidance and efficient battery charging. Transp. Res. C 147, 103995. http://dx.doi.org/10.1016/j.trc.2022.103995, URL https://www.sciencedirect.com/science/article/pii/S0968090X22004089.

Pelletier, S., Jabali, O., Laporte, G., 2019. The electric vehicle routing problem with energy consumption uncertainty. Transp. Res. B 126, 225–255. http://dx.doi.org/10.1016/j.trb.2019.06.006, URL https://www.sciencedirect.com/science/article/pii/S0191261519300153.

Pillac, V., Gendreau, M., Guéret, C., Medaglia, A.L., 2013. A review of dynamic vehicle routing problems. European J. Oper. Res. 225 (1), 1–11. http://dx.doi.org/10.1016/j.ejor.2012.08.015, URL https://www.sciencedirect.com/science/article/pii/S0377221712006388.

Ranasinghe, K., Guan, K., Gardi, A., Sabatini, R., 2019. Review of advanced low-emission technologies for sustainable aviation. Energy 188, 115945. http://dx.doi.org/10.1016/j.energy.2019.115945, URL https://www.sciencedirect.com/science/article/pii/S0360544219316299.

Roosenbrand, E., Sun, J., Hoekstra, J., 2023. Contrail minimization through altitude diversions: A feasibility study leveraging global data. Transp. Res. Interdiscip. Perspect. 22, 100953. http://dx.doi.org/10.1016/j.trip.2023.100953, URL https://www.sciencedirect.com/science/article/pii/S2590198223002002.

Savelsbergh, M.W.P., 1992. The vehicle routing problem with time windows: Minimizing route duration. ORSA J. Comput. 4 (2), 146–154. http://dx.doi.org/10.1287/ijoc.4.2.146, URL https://pubsonline.informs.org/doi/10.1287/ijoc.4.2.146. Publisher: ORSA.

Schiphol, 2023. Developer center. URL https://www.schiphol.nl/en/developer-center/.

Schiphol Health, Safety and Environment office, 2020. Schiphol Regulations. Tech. Rep., Amsterdam, URL https://www.schiphol.nl/en/download/1640595066/43q9kGoE92CccmEeC6awa4.pdf.

Schneider, M., Stenger, A., Goeke, D., 2014. The electric vehicle-routing problem with time windows and recharging stations. Transp. Sci. 48 (4), 500–520. http://dx.doi.org/10.1287/trsc.2013.0490, URL https://pubsonline.informs.org/doi/10.1287/trsc.2013.0490. Publisher: INFORMS.

Soltani, M., Ahmadi, S., Akgunduz, A., Bhuiyan, N., 2020. An eco-friendly aircraft taxiing approach with collision and conflict avoidance. Transp. Res. C 121, 102872. http://dx.doi.org/10.1016/j.trc.2020.102872.

Statistics Netherlands, 2023. Average energy prices for consumers. URL https://www.cbs.nl/en-gb/figures/detail/85592ENG?q=electricity%20price. Last Modified: 2023-12-12T06:30:00+01:00.

Taş, D., 2021. Electric vehicle routing with flexible time windows: a column generation solution approach. Transp. Lett. 13 (2), 97–103. http://dx.doi.org/10.1080/19427867.2020.1711581, Publisher: Taylor & Francis _eprint: https://doi.org/10.1080/19427867.2020.1711581.

Taş, D., Dellaert, N., van Woensel, T., de Kok, T., 2014. The time-dependent vehicle routing problem with soft time windows and stochastic travel times. Transp. Res. C 48, 66–83. http://dx.doi.org/10.1016/j.trc.2014.08.007, URL https://www.sciencedirect.com/science/article/pii/S0968090X1400223X.

Tiseo, I., 2024. Daily European union emission trading system (EU-ETS) carbon pricing from 2022 to 2023. URL https://www.statista.com/statistics/1322214/carbon-prices-european-union-emission-trading-scheme/.

United Nations Framework Convention on Climate Change, 2015. Tech. Rep., United Nations, Paris, URL https://unfccc.int/sites/default/files/english_paris_agreement.pdf.

van Oosterom, S.J., Mitici, M., Hoekstra, J., 2022. Analyzing the impact of battery capacity and charging protocols on the dispatchment of electric towing vehicles at a large airport. In: AIAA AVIATION 2022 Forum. In: AIAA AVIATION Forum, American Institute of Aeronautics and Astronautics, http://dx.doi.org/10.2514/6.2022-3920, URL https://arc.aiaa.org/doi/10.2514/6.2022-3920.

Zhang, L., Liu, Z., Yu, L., Fang, K., Yao, B., Yu, B., 2022. Routing optimization of shared autonomous electric vehicles under uncertain travel time and uncertain service time. Transp. Res. E 157, 102548. http://dx.doi.org/10.1016/j.tre.2021.102548, URL https://www.sciencedirect.com/science/article/pii/S1366554521003069.

Zoutendijk, M., Mitici, M., 2024. Fleet scheduling for electric towing of aircraft under limited airport energy capacity. Energy 294, 130924. http://dx.doi.org/10.1016/j.energy.2024.130924, URL https://www.sciencedirect.com/science/article/pii/S0360544224006960.

Zoutendijk, M., van Oosterom, S., Mitici, M., 2023. Electric Taxiing with Disruption Management: Assignment of Electric Towing Vehicles to Aircraft. AIAA, San Diego.

Zuo, X., Xiao, Y., You, M., Kaku, I., Xu, Y., 2019. A new formulation of the electric vehicle routing problem with time windows considering concave nonlinear charging function. J. Clean. Prod. 236, 117687. http://dx.doi.org/10.1016/j.jclepro.2019.117687, URL https://www.sciencedirect.com/science/article/pii/S0959652619325375.